

The life and times of excited states of organometallic and coordination compounds

Antonín Vlček Jr.^{a,b}

^a *Department of Chemistry, Queen Mary and Westfield College, Mile End Road, London E1 4NS, UK*

^b *J. Heyrovský Institute of Physical Chemistry, Academy of Sciences of the Czech Republic,
Dolejškova 3, CZ-182 23 Prague, Czech Republic*

Received 1 October 1999; accepted 26 January 2000

Contents

Abstract	933
1. Introduction: the two time scales	934
2. What is special about photochemistry of transition metal coordination and organometallic compounds?	938
3. Photochemistry involving long-lived, thermally equilibrated excited states	939
4. Ultrafast photochemistry	948
4.1 Relaxation of the Franck–Condon state	949
4.2 Electron transfer	951
4.3 Intramolecular energy transfer	959
4.4 Ultrafast bond splitting	960
4.5 Coherent phenomena	966
5. Ultrafast, fast, or slow photoprocesses: challenges and perspectives	968
Acknowledgements	971
References	971

Abstract

The photochemistry of transition metal organometallic and coordination compounds is discussed from the perspective of time domains, in which excited-state reactions occur. Ultrafast photochemical processes, which are competitive with nuclear motion, are distinguished from reactions of long-lived, thermally equilibrated, excited states. Many special photochemical features of transition metal complexes and organometallic compounds stem from the simultaneous presence of excited states of different localisations and orbital origins

E-mail address: a.vlcek@qmw.ac.uk (A. Vlček Jr.).

in the same chromophoric molecule, together with high state densities. A brief survey of recently studied systems and reactions shows the present level of understanding and highlights the scientific challenges and possible applications of photoprocesses occurring on different time scales. Factors that influence excited-state lifetimes are discussed and differences in the chemical properties of electronically excited and ground states demonstrated using the radical-like behavior of $[\text{Pt}^{\text{II}}(\text{P}_2\text{O}_5\text{H}_2)_4]^{4-}$ and electron-transfer reactivity of $[\text{Ru}(\text{bpy})_3]^{2+}$ as typical examples. It is shown that reactions of long-lived excited states can become ultrafast when a chromophore is inserted into a redox-active supramolecular assembly or attached to an electrode surface. This has important implications for light-energy conversion and manipulation of information at a molecular level. Optically prepared Franck–Condon excited states of many transition metal complexes have an ultrafast chemistry of their own. This includes relaxation to lower excited states, electron transfer, energy transfer or bond splitting. Typical examples are discussed with an emphasis on phenomena occurring only on very short time scales. A final outlook points to the most challenging questions in mechanistic inorganic photochemistry and to possible applications. © 2000 Elsevier Science S.A. All rights reserved.

Keywords: Photochemistry; Photophysics; Coordination compounds; Organometallics; Ultrafast processes

1. Introduction: the two time scales

The best known natural photochemical processes, photosynthesis and vision, are nature's ways to convert light energy into chemical energy and to capture, store and process optical information. Recent vigorous research in photochemistry and photophysics has essentially the same ultimate goals. On top of that, the pure understanding of chemistry and dynamics of electronic excited states is of a great fundamental importance, not only because of its intellectual appeal but also as an enabling force for the rational design and development of new molecular photonic materials and photochemical reactions. Natural processes of vision and photosynthesis provide a great deal of inspiration. On a very general level, it is important to note that they both operate over a very broad time range¹. The, virtually instantaneous, absorption of a photon is followed by an ultrafast primary photochemical step. For example, the *cis*–*trans* isomerization around a C=C bond of a rhodopsin molecule in the eye's rod cell is completed in about 200 fs (1 fs = 10^{-15} s) [1–4] while the primary electron transfer step in photosynthesis takes some 2–3 ps [5–7]. These ultrafast primary steps are followed by a sequence of much slower thermal reactions, which ultimately accomplish the desired effect. This is clearly demonstrated by the sequence of electron-transfer steps involved in photosynthesis: every subsequent step is slower than the previous one. Ultimately, the charge separation

¹ Kinetic data are in this article reported as 'time constants', defined as reaction lifetimes, which are reciprocal values of the corresponding monomolecular rate constants. The terms 'injection time', 'relaxation time', etc. have the same meaning. If these values are not available, the time needed to complete the discussed process is used instead.

across a photosynthetic membrane is accomplished and the associated free energy used to synthesize ATP and other energy-rich organic molecules. Analogously, in the process of vision, the initial femtosecond isomerization triggers a sequence of thermal steps that ultimately change the flow of Na^+ in ionic channels on a millisecond time scale. Thus, the rate of the dynamic events involved spans some 12 orders of magnitude.

The same principle can be demonstrated (Fig. 1) using $[\text{Ru}(\text{bpy})_3]^{2+}$, perhaps the most studied [8] photoactive coordination compound. Absorption of a photon of visible light takes about 1 fs and prepares the initial, Franck–Condon, excited state. This is the ‘doorway state’ from which the follow-up physical and chemical processes emanate. For $[\text{Ru}(\text{bpy})_3]^{2+}$, it is the spin-singlet metal-to-ligand charge transfer excited state, $^1\text{MLCT}$. Although the electron distribution changes, optical excitation occurs without any change in molecular structure. Hence, the excited state created is far from equilibrium, both internally and with respect to its surroundings. An ultrafast dissipation of the excess of energy follows, producing a long-lived, relaxed, $^3\text{MLCT}$ excited state within ca. 300 fs [9]. This ultrafast energy dissipation is a complex convolution of several processes: vibrational relaxation to an equilibrium geometry of the $^3\text{MLCT}$ state, change of the spin multiplicity, and adjustment of the solvation sphere according to the polarity of the excited molecule. Obviously, the classical textbook picture which views excited-state relaxation as a sequence of steps, that are well-distinguished in time and energy, is completely blurred in the dynamics of the optically prepared excited state of $[\text{Ru}(\text{bpy})_3]^{2+}$ and, in fact, of most transition metal coordination and organometallic complexes. Conventional transition state theory cannot be applied to these ultrafast processes since its basic assumption, i.e. maintaining a Boltzmann equilibrium everywhere along the reaction path, is not fulfilled. The wave packet propagation concept and time-dependent perturbation theory appear to be the most suitable theoretical approaches.

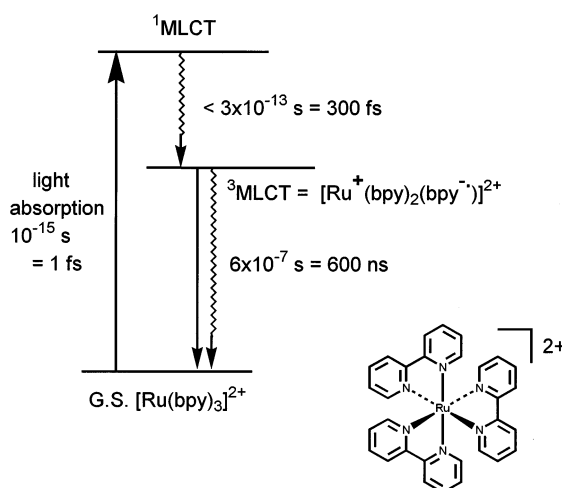


Fig. 1. Photophysics of $[\text{Ru}(\text{bpy})_3]^{2+}$. Vastly different time scales of individual steps involved are stressed out. The complex formula is shown lower-right. G.S. = ground state.

Returning to the $[\text{Ru}(\text{bpy})_3]^{2+}$ example, the long-lived $^3\text{MLCT}$ state, formed by ultrafast relaxation of the $^1\text{MLCT}$ Franck–Condon state, has a photochemistry of its own. It has time to equilibrate into a relaxed geometry and solvent distribution, that is to attain a thermodynamic equilibrium with respect to internal degrees of freedom and to its environment. Its lifetime, 0.6–1 μs , is long enough to allow for diffusion encounters with other species present in solution, opening the much explored area of bimolecular electron transfer photochemistry. It also undergoes slow dissociation of a bpy ligand, by a thermally-activated transition to a dissociative ligand field, LF, excited state [8,10,11]. Thermally equilibrated excited states, of which the $^3\text{MLCT}$ state of $[\text{Ru}(\text{bpy})_3]^{2+}$ is a perfect example, exist in many transition metal complexes [12,13]. They are called THEXI states. A THEXI state is a distinct chemical species in its own right. It can be viewed as an energy-rich isomer of the respective ground state. Unlike ultrafast processes, the chemical reactivity of long-lived, thermally equilibrated excited states (THEXI) are well described by ordinary chemical kinetics, transition state theory and equilibrium thermodynamics. Their equilibrium structure and thermodynamic functions (free energy, redox potentials, $\text{p}K_{\text{a}}$, etc.) are well defined. The distinction between promptly reacting and thermally equilibrated excited states, was recognized in the early 1970s by Adamson [12,13]. Its theoretical consequences were noted shortly afterwards [14]. Notably, this work was done well before first real ultrafast photochemical experiments have been performed.

It is both useful and physically justified to distinguish ‘ultrafast’ photochemical and photophysical processes from slower reactions of thermally equilibrated, long-lived excited states. Different theoretical approaches need to be applied to these two kinds of photoprocesses [14]. But, how fast is ultrafast? An answer to this question clearly depends on the scientific discipline in question, see Fig. 2. Instead of setting exact time limits, it is more appropriate to define ultrafast photochemical processes as those which take place on the time scale of nuclear motion, both intramolecular (vibrations, conformational dynamics) and of the medium (solvation shell, protein or supramolecular surroundings of the chromophore). Translated into time units, the time scale of ultrafast photoprocesses ranges from femtoseconds to, at most, a few hundreds of picoseconds while reactions of relaxed states have lifetimes from several hundreds of picoseconds to microseconds. It is also important to note that ultrafast processes are much faster than diffusion. Hence, they are mostly intramolecular, although ultrafast bimolecular reactions may take place if the reaction partner is present in a very high concentration, especially if it is the solvent. On the other hand, the excited-state lifetime puts much less stringent kinetic limits on reactions of long-lived, relaxed excited states which can show either bimolecular or intramolecular reactivity, or both.

The ubiquity of ultrafast photochemical steps in biological photoprocesses implies that they have some evolutionary advantage over the slower reactions of relaxed excited states. Ultrafast photoreactions are highly directional and selective. Accompanying energy and information losses are minimal, since ultrafast processes are kinetically competitive with any energy-wasting back reactions and side decomposition reactions. Indeed, much current research is focused on the femtosecond

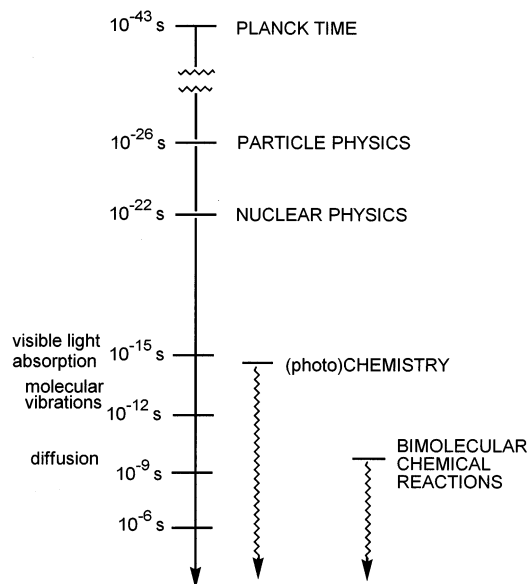


Fig. 2. How fast is ultrafast? Different physical and chemical processes occur on different time scales. Hence, every science would define 'ultrafast' differently. Chemical ultrafast processes concern changes of electronic distribution and motion of atomic nuclei which occur in a femto- to picosecond time domain.

and picosecond dynamics of bacterial or plant photosynthetic centers and the isomerization of rhodopsin or related model compounds. In coordination and organometallic photochemistry, research has traditionally concentrated on the search for long-lived excited states and utilization of their reactions in solar energy conversion or photocatalysis. The emission properties of transition metal compounds and organometallics [15] are pursued especially with regards to their possible applications in sensors [16–19] and probes [20]. Ultrafast photochemical processes of transition metal compounds are less understood, although, their investigation is now gaining much momentum.

The systematic knowledge of photochemistry and photophysics of transition metal complexes is summarized in several books [5,21–23] which build up on the classical text by Balzani and Carassiti published in 1970 [24]. A special issue of *Coordination Chemistry Reviews* (CCR) (vol. 177) has been devoted to various aspects of charge transfer excited states and their photochemistry. Other CCR issues (vols. 132, 159, 171) cover contributions presented at recent International Symposia on Photochemistry and Photophysics of Coordination Compounds. Hereinafter, the photochemistry of coordination and organometallic compounds will be discussed from a different point of view, according to the character and time scale of the early excited-state dynamics involved, with an emphasis on distinctions between ultrafast excited-state reactions and slower photochemistry involving relaxed excited states. The specific features, research challenges, perspectives and

possible applications of photoprocesses occurring on either time scale will be highlighted. The examples used have been chosen only to demonstrate important trends and principles. No attempt is made to cover exhaustively the literature on this enormously broad field.

2. What is special about photochemistry of transition metal coordination and organometallic compounds?

The issue of time scales of excited-state processes is relevant to all photochemistry, regardless of the detailed nature of the photoactive species. However, the presence of a transition metal in a molecule introduces new types of excited states and reactivity patterns which give rise to unique photochemistry and photophysics: (i) Photochemistry of transition metal complexes can often be triggered by irradiation with low-energy visible light since excitation energies are generally lower than in organic compounds. Low-lying, allowed MLCT transitions provide an especially useful gateway through which optical energy is converted into molecular excitation energy. (ii) Transition metal compounds possess various types of excited states, which differ in their orbital parentage, localization within the molecule, energy, dynamics, and reactivity. (iii) The excited state density is much higher than in most organic molecules and several different excited states can occur in a narrow energy range. Hence, excited states of different character can interact with each other, either at the geometry of Franck–Condon (i.e. vertical) excitation or along specific reaction coordinates. This can lead to complex photobehavior which shows competing relaxation and reactivity pathways. Photochemical dynamics and quantum yields often depend on excitation energy and/or temperature due to the presence of energy barriers on photochemical pathways which originate in avoided crossings between excited state potential energy surfaces. (iv) Spin–orbit coupling is strong in metal complexes, especially when second or third row transition metals are present. Consequently, intersystem crossing is fast and its distinction from internal conversion is blurred. However, for practical purposes, it is still possible to use triplet and singlet spin labels, especially for MLCT excited states. (v) Many transition metal complexes are redox-active already in their electronic ground state. Their electron transfer reactions can involve a change in oxidation state of the metal atom, ligand(s) or both. This redox activity is retained in the excited state. Therefore, many metal complexes are prone to photochemical electron transfer reactions. Finally, (vi) great synthetic versatility allows fine-tuning of the excited-state character and energy ordering by judicious structural variations. This point has recently been well demonstrated with $[\text{Re}(\text{E})(\text{CO})_3(\alpha\text{-diimine})]$ and $[\text{Ru}(\text{E})(\text{E}')(\text{CO})_2(\alpha\text{-diimine})]$ complexes [25].

All these aspects make studies of photochemical mechanisms and dynamics of coordination and organometallic compounds very intriguing and challenging, with great potential for discoveries of new phenomena. Importantly, the simultaneous existence of distinct reactivity and relaxation pathways, together with the presence of closely-spaced disparate excited states, provides the possibility to control the

photobehavior of transition metal compounds by external stimuli. This can be especially useful in a development of photonic materials for use as molecular memories or switches. The remarkable connection between excited-state chemistry and electron-transfer reactivity, germane to many transition metal compounds, is very useful both for molecular electronics and light energy conversion.

3. Photochemistry involving long-lived, thermally equilibrated excited states

A long lived excited state, which achieves a thermal equilibrium with respect to internal degrees of freedom and to the medium, differs from the respective ground state in its energy and electron distribution. The higher energy content allows for reactions which are thermodynamically impossible in the ground state. A different electron distribution is responsible for the very different nature, kinetics, and selectivity of excited-state reactions as compared with their ground state counterparts.

This latter point is well demonstrated by bridged dinuclear d^8 – d^8 complexes, namely $[\text{Pt}_2(\text{P}_2\text{O}_5\text{H}_2)_4]^{4-}$, where $\text{P}_2\text{O}_5\text{H}_2^{2-}$ is a μ -pyrophosphito ligand [26–32] (Fig. 3). This complex is very stable and, in its electronic ground state, rather unreactive. It possesses a lowest excited state in which a Pt–Pt bond is created by promoting an electron from an antibonding $d(\sigma^*)$ orbital into a bonding $p(\sigma)$ orbital (Fig. 3) [33,34]. The $^3d(\sigma^*)p(\sigma)$ excited state shows a strong green emission whose decay reveals a very long excited-state lifetime, about 10 μs . Besides being a strong photochemical reductant and oxidant, $[\text{Pt}_2(\text{P}_2\text{O}_5\text{H}_2)_4]^{4-}$ in its $^3d(\sigma^*)p(\sigma)$

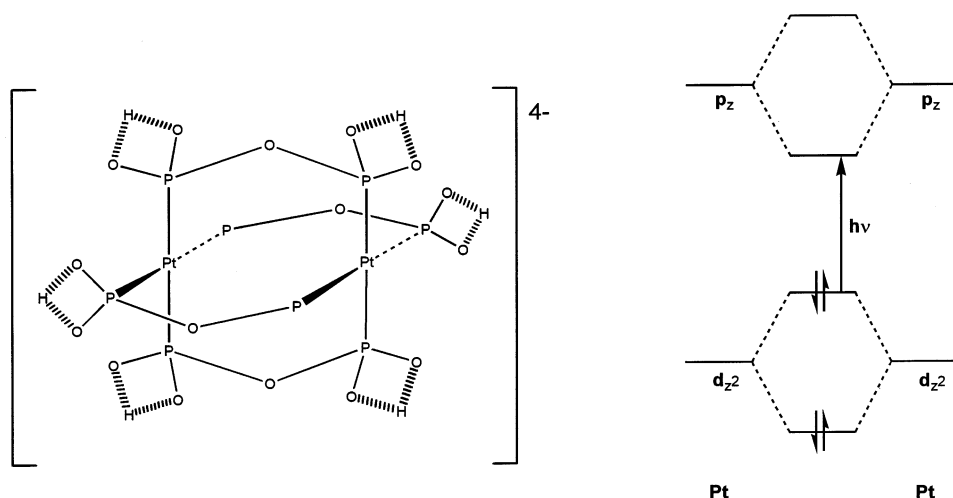


Fig. 3. Structure (left) and simplified molecular orbital scheme (right) of $[\text{Pt}_2(\text{P}_2\text{O}_5\text{H}_2)_4]^{4-}$. It follows that $d(\sigma^*) \rightarrow p(\sigma)$ excitation leads to a Pt–Pt bonding interaction. (The $-\text{O}\cdots\text{H}\cdots\text{O}-$ groups at one of the P atoms of each equatorial $\text{P}_2\text{O}_5\text{H}_2^{2-}$ ligand were omitted for clarity.)

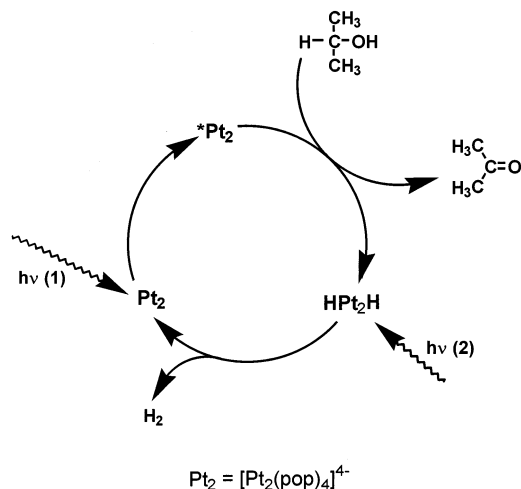


Fig. 4. Two-photon photocatalytic dehydrogenation of isopropanol to acetone using $[\text{Pt}_2(\text{P}_2\text{O}_5\text{H}_2)_4]^{4-}$ as a photocatalyst.

excited state behaves essentially as a free radical, abstracting H-atoms from isopropanol [28,31,32,35] or organometallic hydrides Ph_3MH , $\text{M} = \text{Si}, \text{Ge}, \text{Sn}$ [36,37]. The deuterium kinetic isotope effect found for the latter reaction is characteristic of an atom transfer reaction [36,37]. Moreover, rate constants of hydrogen abstraction from Ph_3MH by the $^3\text{d}(\sigma^*)\text{p}(\sigma)$ excited state of $[\text{Pt}_2(\text{P}_2\text{O}_5\text{H}_2)_4]^{4-}$ and by a ground-state butoxy radical $^t\text{BuO}^\bullet$ depend on M in the same way. This radical-like behavior of $^3\text{d}(\sigma^*)\text{p}(\sigma)$ state of $[\text{Pt}_2(\text{P}_2\text{O}_5\text{H}_2)_4]^{4-}$ and analogous dinuclear $\text{d}^8\text{--d}^8$ complexes stems from the single-occupancy of the $\text{d}(\sigma^*)$ orbital, which is localized on Pt atoms, pointing out of the molecule. In the electronic ground state, this orbital is doubly occupied. The chemistry of $[\text{Pt}_2(\text{P}_2\text{O}_5\text{H}_2)_4]^{4-}$ thus changes upon excitation from that of a weak Lewis base to radical-like. The ability of a $^3\text{d}(\sigma^*)\text{p}(\sigma)$ excited state to abstract H-atoms makes $[\text{Pt}_2^{\text{II}}(\text{P}_2\text{O}_5\text{H}_2)_4]^{4-}$ a very interesting photocatalyst. Shown in Fig. 4 is a two-photon catalytic dehydrogenation of isopropanol to acetone. Absorption of the first photon produces the $^3\text{d}(\sigma^*)\text{p}(\sigma)$ state which abstracts the first H-atom. Eventually, a $[\text{Pt}_2^{\text{III}}(\text{H})_2(\text{P}_2\text{O}_5\text{H}_2)_4]^{4-}$ dihydride [35] is produced. Upon absorption of a second photon, the dihydride undergoes a reductive elimination of H_2 , regenerating the $[\text{Pt}_2^{\text{II}}(\text{P}_2\text{O}_5\text{H}_2)_4]^{4-}$ photocatalyst. The ability of $[\text{Pt}_2^{\text{II}}(\text{P}_2\text{O}_5\text{H}_2)_4]^{4-}$ and $[\text{Pt}_2^{\text{III}}(\text{H})_2(\text{P}_2\text{O}_5\text{H}_2)_4]^{4-}$ to photochemically abstract and transfer H-atoms, respectively, is the basis of dehydrogenation and hydrogenation photocatalytic reactions of hydrocarbons [29–32,38] and, even, DNA [39].

There are many other examples of photoactive dinuclear $\text{d}^8\text{--d}^8$ complexes of Pt, Rh or Ir. Most of them photochemically abstract halide atoms from organic halides [28,30,31]. Dinuclear iridium(I) complexes containing two bridging pyrazolyl ligands, $[\text{Ir}_2(\mu\text{-pz})_2(\text{CO})_2(\text{PR}_3)_2]$, are especially worth mentioning since they also

undergo reversible electron transfer reactions. Both the singlet and triplet $d(\sigma^*)p(\sigma)$ excited states of these Ir_2 complexes can be quenched by suitable oxidants [40]. While the 100 ps lifetime of the singlet state allows only for an intramolecular electron transfer with electron acceptors covalently attached to the phosphine ligands, the triplet state ($\tau \approx 1 \mu\text{s}$) can also react bimolecularly, with oxidants present in the solution. Investigations of these electron transfer reactions have contributed much to the understanding of electron transfer reactivity [40–43], including the first observation of a Marcus inverted effect on bimolecular electron transfer [44].

Another type of long-lived excited states, $\delta\delta^*$, arises from the metal–metal quadruple bond present in dinuclear complexes of the type $[\text{Re}_2\text{Cl}_8]^{2-}$ or $[\text{Mo}_2\text{X}_4(\text{PR}_3)_4]$ [45–48]. Quite unusually, spin-singlet $\delta\delta^*$ states have much longer lifetimes than corresponding triplets do. This is caused by a very large singlet–triplet splitting, combined with a small energy gap between the triplet state and the ground state. Bimolecular excited-state electron transfer reactions are typical for Re_2 complexes [49] while their Mo_2 or W_2 analogues have been implicated [48] in oxidative additions and two-electron redox reactions. However, some photoreactivity of the latter species originates in upper, short-lived excited states [48,50].

Porphyrin complexes of various metals represent another broad class of compounds with long-lived excited states. They have been widely used in excited-state electron- and energy-transfer processes, and as photocatalysts or sensitizers in light-energy conversion [51–53]. Recently developed [54,55] complexes of the general type $[\text{Pt}(\text{dithiolate})(\alpha\text{-diimine})]$ have long-lived excited states of a dithiolate $\rightarrow \alpha\text{-diimine}$ ligand-to-ligand charge transfer (LLCT) origin. They show rich excited-state redox chemistry and have a great potential for further applications.

Owing to its long-lived excited state, $[\text{Cp}^*\text{Ir}(\text{H})(\alpha\text{-diimine})]^+$ is the active species in photocatalyzed water gas shift reaction [56,57]. Its excited state has a lifetime of 80 or 190 ns for $\alpha\text{-diimine} = \text{bpy}$ or phen , respectively [58]. It reacts with H^+ in aqueous solution to produce H_2 and, in the presence of Cl^- ions, $[\text{Cp}^*\text{Ir}(\text{Cl})(\text{bpy})]^+$. Originally, an $\text{Ir} \rightarrow \text{bpy}$ MLCT excited state was supposed [58] to be the reactive state. However, a $\text{Cp}^{*-} \rightarrow \text{bpy}$ LLCT or $(\text{Ir}-\text{H}) \rightarrow \text{bpy}$ sigma-bond-to-ligand charge transfer, SBLCT, state are other likely candidates. The detailed mechanism of this photochemical reaction remains unclear.

Some complexes with long-lived excited states undergo relatively slow photochemical metal–ligand bond dissociation or homolysis. For example, irradiation of $[\text{Re}(\text{benzyl})(\text{CO})_3(^i\text{Pr-DAB})]$ or $[\text{Ru}(\text{SnPh}_3)_2(\text{CO})_2(^i\text{Pr-DAB})]$; $^i\text{Pr-DAB} = ^i\text{Pr}-\text{N}=\text{CH}-\text{CH}=\text{N}^i\text{Pr}$; populates a $^3\text{SBLCT}$ state from which Re-benzyl or Ru-SnPh_3 bond homolysis occurs with rather long lifetimes of 250 ns and ca. 1 μs , respectively [59–61]. Interestingly, the Re-benzyl bond homolysis becomes ultrafast, presumably subpicosecond, on changing the solvent from toluene to more polar and donating THF or CH_3CN [59,60]. Substituting the $^i\text{Pr-DAB}$ ligand for bpy makes the bond homolysis ultrafast, regardless of the solvent, vide infra [62,63]. Another example of a ligand dissociation from a relaxed excited state is provided [64] by Werner-type d^6 $\text{Rh}(\text{III})$ complexes. Their $t_{2g} \rightarrow e_g$ LF excited state undergoes dissociative ligand substitution on a nanosecond time scale. However, although

‘slow’ from the photochemical point of view, the LF excited-state reaction is about 10^{15} -times faster than the corresponding ground state reaction. Moreover, the ligand selectivity is different. However, these examples are rather exceptional. In fact, photochemical bond splitting from long-lived excited states is a rare process. It usually occurs with an ultrafast rate from Franck–Condon excited states, as will be discussed in the next section.

By far, the best known and most studied long-lived excited state is that of $[\text{Ru}(\text{bpy})_3]^{2+}$ [8,10,11,26,51,65–68]. The discovery that its emissive $^3\text{MLCT}$ excited state undergoes bimolecular electron transfer reactions in fluid solution [69] has opened a whole new field of inorganic photochemistry. Similar behavior is shown by Ru complexes with other polypyridyl ligands (N,N), their Os analogues, bis-polypyridyl complexes $[\text{M}(N,N)_2(\text{X})(\text{Y})]^\pm$; $\text{M} = \text{Ru}, \text{Os}$; $[\text{Cu}(N,N)_2]$ [70], or $[\text{Re}(\text{L})(\text{CO})_3(N,N)]$ [21]. In general terms, the unique behavior of all these complexes originates in the combination of their redox activity with the presence of a low-lying, long-lived excited state.

In its electronic ground state, $[\text{Ru}^{\text{II}}(\text{bpy})_3]^{2+}$ can be both oxidized and reduced by one electron to $[\text{Ru}^{\text{III}}(\text{bpy})_3]^{3+}$ and $[\text{Ru}^{\text{II}}(\text{bpy})_2(\text{bpy}^{\bullet-})]^+$, respectively. Its relaxed $^3\text{MLCT}$ excited state can be formulated as $[\text{Ru}^{\text{III}}(\text{bpy})_2(\text{bpy}^{\bullet-})]^{2+}$, simultaneously containing an oxidizing Ru(III) and reducing $\text{bpy}^{\bullet-}$ sites. Indeed, the $^3\text{MLCT}$ excited state of $[\text{Ru}^{\text{II}}(\text{bpy})_3]^{2+}$, abbreviated $^*[\text{Ru}^{\text{II}}(\text{bpy})_3]^{2+}$, is a strong reductant as well as oxidant. This has been amply demonstrated by numerous studies of reductive and oxidative quenching of $[\text{Ru}^{\text{II}}(\text{bpy})_3]^{2+}$ phosphorescence. In fact, even the nonradiative decay of $^*[\text{Ru}^{\text{II}}(\text{bpy})_3]^{2+}$ to the ground state can be viewed as an intramolecular electron transfer reaction: $\text{bpy}^{\bullet-} \rightarrow \text{Ru}(\text{III})$. Systematic investigations of the nonradiative decay rate of MLCT excited states of Ru(II), Os(II), and Re(I) complexes as a function of the driving force, molecular structure, and medium have highlighted the analogy with electron transfer in Marcus inverted region. Factors determining excited-state lifetimes and electron transfer rates are now well understood. Namely, the concept of the energy gap law has been highly elaborated and introduced into inorganic and organometallic photochemistry [71–77]. An energy gap between the excited and ground state, structural rigidity, and the extent of delocalization of an excited electron over the acceptor ligand are the most important factors affecting lifetimes of MLCT excited states. The latter two factors can even compensate for a small energy gap. On the other hand, the presence of short-lived, higher-lying LF excited state can seriously diminish MLCT excited-state lifetimes, especially if the MLCT and LF states are close in energy. Detailed understanding of these relations now allows to design complexes which absorb even low energy visible light while still possessing long-lived excited states [75,76].

The quest for polypyridyl complexes with very long-lived excited states started immediately after the discovery of their bimolecular redox reactivity. It was driven both by curiosity, attempting to actually ‘see’ excited molecules, and by the need to improve yields of excited-state bimolecular electron transfer reactions diminished by the inevitable competition with excited-state decay. The development of polypyridyl complexes with long-lived excited states still continues, despite the fact that the

interest in bimolecular electron transfer reactions has somewhat abated. The synthesis [78,79] of a rigid caged derivative of $[\text{Ru}^{\text{II}}(\text{bpy})_3]^{2+}$, in which all three bpy ligands are covalently linked together, was one of the milestones on the way to photosensitizers with long-lived excited states. Compared with $[\text{Ru}^{\text{II}}(\text{bpy})_3]^{2+}$, the caged derivative has about twice longer excited-state lifetime (1.7 μs) and its photostability is much improved. Recognition of the importance of the extensive delocalization of the excited electron over the ligand π -system was another essential step forward [75,76]. Extending the delocalization by attaching a $-\text{C}=\text{C}-$ group to the 4-position of the bpy ligand seems to be an especially efficient strategy: microsecond lifetimes were found [75] for Ru(II) complexes containing 4-vinyl-bpy ligand or mono- and di-nuclear Ru(II) complexes of bbpe (Fig. 5). Ru(II) terpyridine (trpy) complexes have much shorter-lived excited states than their bpy counterparts because of increased molecular distortion in the excited state and small energy gap between the $^3\text{MLCT}$ and the short-lived LF excited state which lies at only slightly higher energy. However, excited-state lifetimes are much longer [81–83] in dinuclear complexes $[(\text{trpy})\text{Ru}(\text{trpy-B-trpy})\text{Ru}(\text{trpy})]^{4+}$ where the electron delocalization is extended through the bridging group B ($-\text{C}\equiv\text{C}-$ or p -phenylene) attached to the 4-position of the trpy central pyridine rings (Fig. 5). This approach is being used [82,83] to construct photoactive supermolecular assemblies and molecular wires. Still another strategy [84] to the construction of molecules with long-lived MLCT states involves attaching a strongly electron-accepting pyridinium group directly to a bpy or 1,10-phenanthroline ligand (Fig. 5) in complexes of the type $[\text{Ru}^{\text{II}}(\text{phen})_2(\text{phen-py}^+)]^{3+}$. Instead of the expected intramolecular quenching of the MLCT state, an extension of its emission lifetime was found. It remains a question whether the excited electron is delocalized over the phen-py $^+$ ligand or fully transferred to its pyridinium part. Last, but very efficient, strategy to prolong MLCT excited-state lifetimes relies on a coupling with a long-lived intraligand state. For example, excited-state lifetime of $[\text{Ru}^{\text{II}}(\text{bpy})_3]^{2+}$ derivatives in which a pyrene unit is covalently attached to one bpy ligand is 42 μs [80].

Long-lived charge separation can also be accomplished in various molecular triads [5] in which an electron donor and acceptor are simultaneously bound to a redox-active chromophore. Such triads are often built around a central porphyrin or metal-polypyridyl unit. Long-lived charge separation is produced stepwise, involving fast or even ultrafast electron transfer from an optically prepared excited state, vide infra. $[\text{Re}(\text{BPP})(\text{CO})_3(\text{DEAS-bpy})]^+$, shown in Fig. 6, is a very interesting example [85,86]. Optical excitation of this complex ultimately produces a charge-separated state $[\text{Re}(\text{BPP}^{\bullet-})(\text{CO})_3(\text{DEAS-bpy}^{\bullet+})]^+$, which has a lifetime of 4.3 μs . It can be viewed formally as a ligand-to-ligand charge transfer excited state. Other interesting coordination compounds capable of intramolecular charge separation are derived [87] from $[\text{M}(\text{trpy})_2]^{2+}$; $\text{M} = \text{Ru}$ or Os ; by attaching an p -phenyltriarylpyridinium or MV^{2+} group to one terpyridine ligand and a $\text{Me}_2\text{N-}p$ -phenyl group to the other (Fig. 6).

The continuing development of complexes which can be optically excited into a long-lived excited or charge-separated state has largely been motivated by their

possible use in solar energy conversion. Separated reducing and oxidizing sites can react with other substrates, converting them to highly energetic products. For example, $[\text{Ru}(\text{bpy})_3]^{2+}$ in its $^3\text{MLCT}$ excited state has the right redox potentials to reduce and oxidize water to H_2 and O_2 respectively [88–91]. Fig. 7 shows a possible,

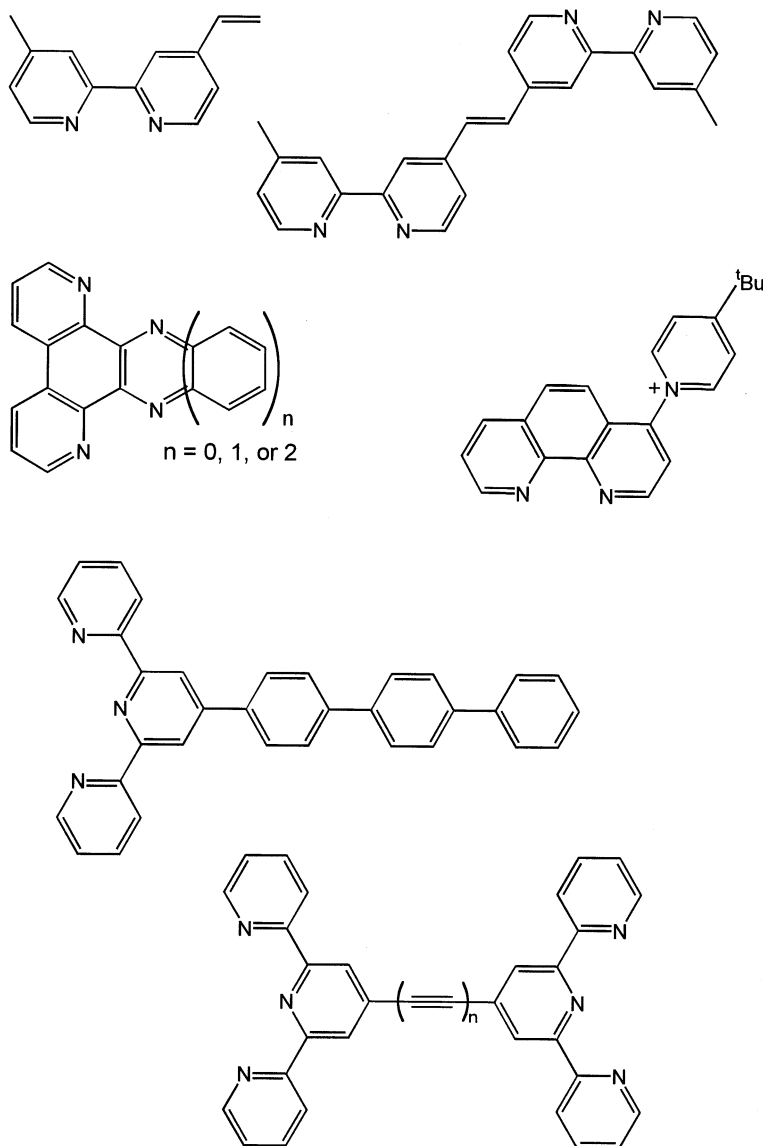


Fig. 5. Examples of ligands capable of prolonging lifetimes of MLCT excited states by extended delocalization of the excited electron [75,76,84]. The bbpe ligand is shown top-right.

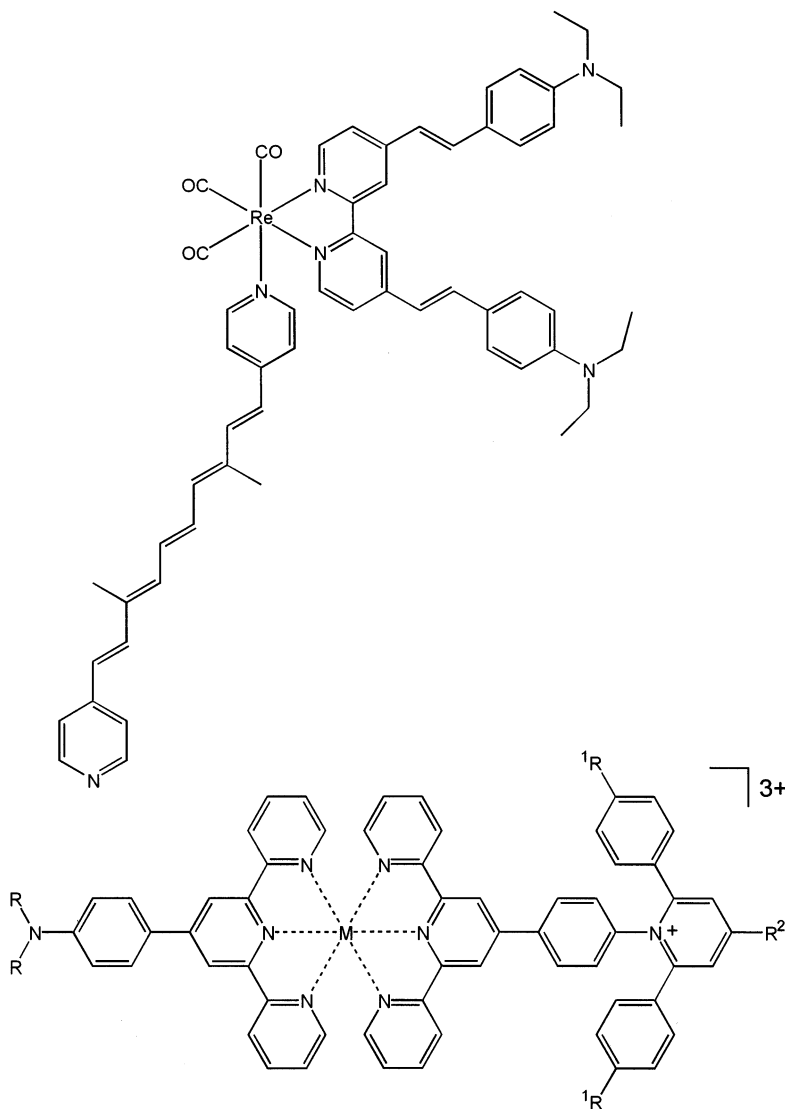


Fig. 6. Examples of complexes whose MLCT excitation leads to a long-lived charge separation. Top: $[\text{Re}(\text{BPP})(\text{CO})_3(\text{DEAS-bpy})]^+$ [85,86]. Bottom: $[(\text{Me}_2\text{N-p-phenyl-trpy})\text{M}(\text{p-phenyl-triarylpyridinium-trpy})]^{3+}$; M = Ru or Os; [87].

albeit idealized, photocatalytic scheme for water splitting. If working efficiently, such a photocatalytic process would have a great practical and economical impact. An enormous research effort has been invested in development of artificial photosynthesis. The main problems of homogeneous schemes like that shown in Fig. 7

are various cross reactions which severely diminish the process efficiency. Firstly, it is the decay of an excited state to the ground state, which is often competitive with the forward electron transfer reaction that leads to charge separation. As was discussed above, Nature overcomes this problem in bacterial and plant photosynthesis by using an ultrafast, vectorial electron transfer in a highly organized supramolecular assembly of chromophores, electron acceptors and donors, instead of simple homogeneous bimolecular reactions. Despite this, complexes with long-lived excited states were traditionally believed to be the most promising sensitizers for artificial systems. The second main drawback is the presence of a back reaction, which can be compared to an electrical short circuit. In the particular case shown in Fig. 7, one can easily imagine a fast back reaction between an oxidized $[\text{Ru}(\text{bpy})_3]^{3+}$ complex and reduced methylviologen radical, $\text{MV}^{\bullet+}$, that would simply regenerate corresponding starting species, without accomplishing any useful chemical transformation. Nature's way to overcome back reactions is to drive the forward electron transfer through a redox cascade with only small driving force per redox step, while back reactions are slow because of the inverted effect of their huge driving force. Spatial organization of the photosynthetic reaction center is of a paramount importance in defining redox pathways. Both strategies—that is engineering of systems whose back reactions would occur with a high driving force in the Marcus inverted region and organizing/separating the oxidants and reductants at phase boundaries of micelles, bilayers, membranes, etc.—were used in a development of artificial systems. The third problem concerns the stability of components of photocatalytic systems. The longer the excited states live, the greater chance they have to undergo unwanted decomposition or side reactions with other components of the system. For example, $[\text{Ru}(\text{bpy})_3]^{2+}$ slowly loses a bpy ligand on irradiation. The same is true for strong oxidants and reductants involved in photocatalytic cycles. For instance, the long-term efficiency of artificial photosynthetic systems related to that shown in Fig. 7 is severely limited by hydrogenation of bpy and

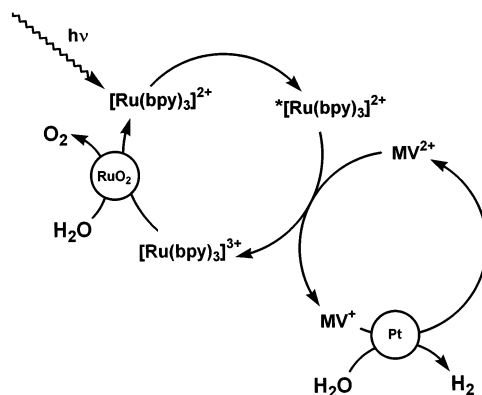


Fig. 7. Idealized scheme of a photocatalytic water splitting using $[\text{Ru}(\text{bpy})_3]^{2+}$ as a sensitizer. MV^{2+} : methylviologen. Pt, RuO_2 : colloidal catalysts of water reduction and oxidation, respectively.

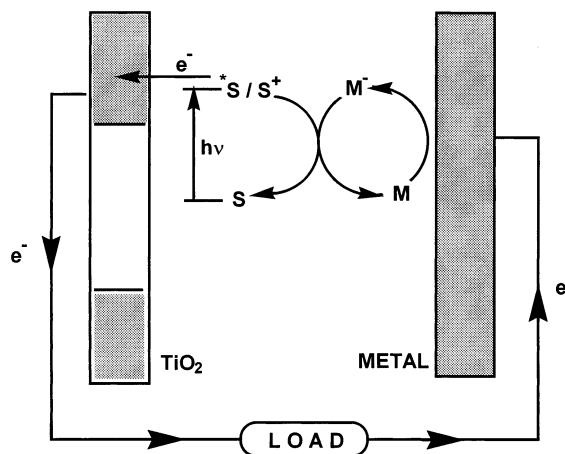


Fig. 8. Photoelectrochemical solar cell based on a sensitized TiO_2 electrode. S: sensitizer, M: redox mediator.

MV^{2+} in the presence of colloidal platinum. Intensive research on these problems has greatly advanced our knowledge of excited state deactivation and of homogeneous, intramolecular, and heterogeneous electron transfer reactions. However, no durable and practical homogeneous or microheterogeneous system of photochemical light energy conversion has yet been developed. Conventional methods to improve efficiency are often mutually incompatible. For example, sensitizers with longer-lived excited states often capture less light energy and/or are less photochemically stable. One way out of this dilemma would be to employ ultrafast electron transfer reactions in organized supramolecular systems as a primary step, instead of diffusion-limited bimolecular ones. Another promising direction is to abandon homogeneous or microheterogeneous systems and switch to photoelectrochemistry at semiconductors [88,92–94].

Fig. 8 shows schematically photoelectrochemical light conversion using a typical and most convenient semiconductor, TiO_2 –anatase. In principle, electron can be excited directly from the semiconductor's valence band into its conduction band, followed by passage of current to a counter electrode. The circuit is closed with a suitable redox mediator M that transfers the electron back to the semiconductor. In this way, light energy is converted to electrical energy. The problem with TiO_2 is, that it does not absorb light in the visible spectral region, which makes it unsuitable for applications in solar energy conversion. This drawback can be overcome (Fig. 8) by using a sensitizer S, that is a photoactive compound which can be excited by visible light and then transfers electron directly to the conduction band of the semiconductor electrode. A good sensitizer should absorb light efficiently throughout the visible spectral region, its $^*\text{S}/\text{S}^+$ excited-state redox potential has to be above the edge of the conduction band, it should hold at the surface of the semiconductor, and transfer the electron as quickly as possible. Moreover, both the

sensitizer S and its oxidized form S^+ should be stable. Many polypyridyl transition metal complexes as well as some organic dyes proved to be good and efficient sensitizers. The best sensitizers known [92] at the time of writing are $[\text{Ru}(\text{bpy}-4,4'-(\text{COOH})_2)_2(\text{NCS})_2]$ and $[\text{Ru}(\text{trpy}-2,2',2''-(\text{COOH})_3)(\text{NCS})_3]^-$. The $-\text{COOH}$ groups guarantee a strong adsorption to the surface of a TiO_2 electrode while NCS^- ligands shift light absorption to long wavelengths and provide good photochemical stability. The electron transfer occurs from a MLCT excited state. Solar cells constructed by Grätzel et al. using the sensitizer $[\text{Ru}(\text{bpy}-4,4'-(\text{COOH})_2)_2(\text{NCS})_2]$ achieve an efficiency of nearly 10% and have reasonable long-term stability [92].

Initially, the search for good sensitizers concentrated on species with long-lived excited states, in the belief that long excited-state lifetimes are needed for electron transfer to be competitive with decay to the ground state. However, this all changed with a groundbreaking discovery [95–97] that interfacial electron transfer from an excited sensitizer to TiO_2 is an ultrafast process, completed in 25–150 fs! Such a fast rate is competitive with any nonradiative excited-state decay or decomposition. This discovery dispensed with the myth that complexes with long-lived excited states are superior in photochemical or photoelectrochemical light-energy conversion. Suddenly, it became obvious that the search for potential sensitizers need not to be restricted to compounds with long-lived excited states. Indeed, $[\text{Fe}(\text{bpy}-4,4'-(\text{COOH})_2)_2(\text{CN})_2]$, whose MLCT excited-state lifetime is only ca. 330 ps, was found [98] to act as a sensitizer in a TiO_2 -based solar cell. In fact, even the classical Grätzel cell would not operate as well as it does if the interfacial electron transfer were not ultrafast, since the $[\text{Ru}(\text{bpy}-4,4'-(\text{COOH})_2)_2(\text{NCS})_2]$ sensitizer has a natural excited-state lifetime of only 50 ns.

4. Ultrafast photochemistry

Optical excitation, which takes place in about 1 fs, prepares a Franck–Condon excited state. This is an electronically excited state which, because of the ‘vertical character’ of electronic excitation, retains the geometry of the ground state. Hence, the Franck–Condon states are, in most cases, excited both electronically and vibrationally and molecular surroundings are in a highly nonequilibrated configuration. Energy dissipation inevitably follows optical excitation. It can occur as a relaxation to lower-lying excited state(s), or as a chemical reaction, usually bond splitting or electron transfer. If both the reactive and relaxation channels are open, branching of the Franck–Condon state evolution occurs. The corresponding branching ratio is the principal factor determining the photochemical quantum yield [63,99,100]. Lower excited states, populated nonradiatively from the Franck–Condon excited state, can also undergo ultrafast reactions or they equilibrate into long-lived excited states. Hereafter, selected ultrafast reactions and phenomena observed in the photochemistry of coordination and organometallic compounds will be briefly surveyed and their more intriguing and general points will be stressed out.

4.1. Relaxation of the Franck–Condon state

Classical photochemistry textbooks offer a neat picture of energetically and temporally well-separated relaxation steps: vibrational relaxation followed by internal conversion to the lowest singlet state, followed by still slower intersystem crossing to the lowest triplet, which undergoes a chemical reaction, phosphoresces, or just decays nonradiatively to the ground state. However, relaxation of higher excited states of transition metal complexes only rarely conforms to this picture. Lowest stable excited states or primary photoproducts are often formed extremely rapidly, in subpicosecond processes, and without any discernible intermediate states. There are many examples of such behavior. As was mentioned above, intersystem crossing, vibrational and solvent (CH_3CN) relaxation of the optically prepared $^1\text{MLCT}$ excited state of $[\text{Ru}(\text{bpy})_3]^{2+}$ to the long-lived $^3\text{MLCT}$ state occur [9] in a single process, completed in 300 fs. The time constant of the $^1\text{MLCT} \rightarrow ^3\text{MLCT}$ has been determined [101] for an analogous $[\text{Ru}(\text{dmb})_3]^{2+}$ complex as 120 fs ($\text{dmb} = 4,4'$ -dimethyl-2,2'-bpy). Other examples show that a specific lower excited state can be populated in a single ultrafast step from a higher-lying state, even if other excited states lie between them. For example, optical excitation of low-spin Fe(II) polypyridyl complexes into their $^1\text{MLCT}$ state is followed by a conversion into the $^5\text{T}_2$ metal-centered LF excited state which is completed in less than 700 fs with a 100% efficiency. Notably, this process is ultrafast despite its strongly spin-forbidden character ($\Delta S = 2$) [102]. The $^3\text{MLCT}$ and $^3\text{T}_2$ excited states, which lie between the $^1\text{MLCT}$ and $^5\text{T}_2$ states, are apparently bypassed during $^1\text{MLCT}$ state relaxation. Ultrafast optical conversion of low-spin Fe(II) complexes into a high-spin $^5\text{T}_2$ excited state is the basis of optical switching of magnetic properties of Fe(II) compounds [103,104]

Similarly, the $^1\text{T}_1$ and $^5\text{T}_2$ metal-centered states of Co(III) ammine complexes have been found [105] to be populated from the optically excited $^1\text{LMCT}$ state in less than 700 fs, apparently bypassing the corresponding triplet states. Another case of an ultrafast relaxation of a LMCT excited state is represented by the Cu center of the blue copper protein plastocyanin [106]. In this case, however, electronic relaxation proceeds stepwise: The optically prepared (cystein-S) $\rightarrow \text{Cu}^{2+}$ LMCT state relaxes with a lifetime of 125 fs to a lower-lying LF excited state, which subsequently decays to the ground state with a lifetime of 285 fs.

Only little information on vibrational relaxation of excited coordination complexes is available. For the molecules discussed in the preceding paragraph, there is no evidence for vibrational cooling prior to electronic relaxation. It appears that vibrational and electronic relaxation either occur as a single step or that vibrational excitation is carried over to the products, through electronic relaxation or a reaction of the Franck–Condon state. Indeed, lower excited states or a ground state formed by ultrafast electronic relaxation are often initially produced in higher vibrational levels (vibrationally hot). Slower vibrational relaxation follows afterwards. This has been observed for the $^5\text{T}_2$ state of some Fe(II) polypyridyl complexes [102], as well as for photochemically produced ground state deoxyhemoglobin [107] and myoglobin [108], and a series of binuclear $[\{\text{Re}(\text{CO})_3\text{Cl}\}_2(\mu\text{-polypyridyl})]$ complexes

[109]. Time constants of vibrational relaxation of these species are in the range 2–10 ps. No vibrational relaxation has been observed for $[\text{Ru}(\text{bpy})_3]^{2+}$. On the other hand, $^1\text{MLCT} \rightarrow ^3\text{MLCT}$ intersystem crossing of analogous $[\text{Ru}(\text{dmb})_3]^{2+}$ is followed by vibrational relaxation of the $^3\text{MLCT}$ state formed. It occurs with a time constant of 5 ps [101]. Interestingly, formation of the $\text{Ru} \rightarrow \text{dpb}$ $^3\text{MLCT}$ excited state of $[\text{Ru}(\text{dpb})_3]^{2+}$; $\text{dpb} = 4,4'$ -diphenyl-2,2'-bpy; is accompanied by a rotation of the phenyl rings whose time constant is ca. 2 ps [101].

Slower vibrational relaxation was found for metal carbonyls: Time constants in the range 10–40 ps were measured [110] for vibrational relaxation of a CO ligand bound to metalloporphyrins. Many photochemical reactions of metal carbonyls occur faster than and/or competitively with vibrational relaxation, often producing vibrationally excited products, whose relaxation can then be studied. For example, excitation of $\text{Cr}(\text{CO})_6$ triggers femtosecond production of $[\text{Cr}(\text{CO})_5(\text{S})]$, while some $\text{Cr}(\text{CO})_6$ is recovered. Both these species are initially formed vibrationally excited and undergo vibrational relaxation with a time constant of 20–30 and 110 ps, respectively [172]. The solvent-dependence of vibrational relaxation of low-frequency vibrational modes by energy transfer to solvent has been studied [111] for $[\text{Rh}(\text{CO})(\text{acetylacetonate})]$ photoproduced from $[\text{Rh}(\text{CO})_2(\text{acetylacetonate})]$. The time constant was found to increase from 5 to 18 ps on going from *n*-hexane to CCl_4 .

In conclusion, vibrational relaxation, electronic relaxation and changes of spin multiplicity can occur in electronically excited coordination and organometallic compounds as a single, convoluted process, defined by the initial and final electronic states. By and large, this behavior indicates a high degree of electronic and vibronic coupling between the Franck–Condon state and lower electronic states along respective relaxation coordinates. This coupling apparently creates channels on excited-state potential energy surfaces along which excited wave packets evolve directly into the final state. The conventional ‘ladder’ type scheme of excited-state dynamics is not applicable. Photoproducts and lower electronic states are often formed vibrationally excited. Ultimately, the excess energy is transferred to the solvent bath. Hence, the connection between solvation dynamics and excited-state relaxation also deserves comment. Femtosecond studies of dynamic solvent effects have revealed [112,113] that solvent dynamics cannot be characterized by a single time constant. The longitudinal solvent relaxation time is, in most cases, too long to be of importance in the ultrafast decay of an excited solute molecule. It appears [112,114,115] that it is the inertial solvent relaxation which is coupled to ultrafast excited-state dynamics. The inertial solvent movement, which corresponds to an uncorrelated rotational movement of solvent molecules in the first solvation sphere, is very fast. For example, an inertial relaxation time of 100 fs was determined [112] for CH_3CN . Water or CH_2Cl_2 behave similarly.

In metalloproteins, it is the protein surroundings which first absorb the excess energy dissipated during relaxation of an excited metal-containing chromophore. In a follow-up step, the protein has to relax itself, usually in a multi-phasic process, with the fastest component occurring on the time scale of picoseconds or even less. Such fast protein relaxation dynamics were observed for hemes [116,117] as well as blue copper proteins [106,118].

4.2. Electron transfer

At the end of Section 3, it was discussed how research on artificial light energy conversion took a new twist by the breakthrough discovery that interfacial electron transfer at a semiconductor surface is an ultrafast process. In particular, it was found that electron transfer from a MLCT excited state of a typical $[\text{Ru}(\text{bpy}-4,4'-(\text{COOH})_2)(\text{NCS})_2]$ sensitizer into the conduction band of colloidal or thin film TiO_2 takes place with a time constant of about 50 fs in a colloidal solution [95,119,120] and less than 25 fs in high vacuum [122]. Some studies have indicated biphasic kinetics, with a minor component of about 1 ps. Similar ultrafast electron injection was found to occur also from an inherently short-lived MLCT excited state of $[\text{Fe}(\text{bpy}-4,4'-(\text{COOH})_2)_2(\text{CN})_2]$ [98], and $[\text{Fe}(\text{CN})_6]^{4-}$ [122] or from various organic dyes [96,97,123–125] or porphyrins [127]. Ultrafast electron injection is hardly affected by the medium: it was observed both in solution and high vacuum. Its rate is also independent of temperature over a broad range (22–300 K, in vacuum [97]). The strong adsorption of a sensitizer molecule to the TiO_2 surface via various anchoring groups ($-\text{COOH}$, $-\text{P}(\text{O})(\text{OH})_2$, $-\text{CN}$, $-\text{OH}$, etc) is common to all these systems. An interesting question arises, as to what extent the excited state is delocalized between the sensitizer molecule and the semiconductor. This question can be posed in another way: whether electron-injection into the semiconductor is a real electron transfer reaction, temporally separated from the optical transition, or whether it should better be viewed as direct optical excitation into a semiconductor? It appears that these two possibilities represent only extreme, limiting cases. The actual extent of electronic delocalization between the sensitizer and TiO_2 depends on the anchoring group. For $[\text{Ru}(\text{bpy}-4,4'-(\text{COOH})_2)(\text{NCS})_2]$, it was argued that electron injection is distinct from the optical excitation, despite its ultrashort duration; < 25 fs [121]. This is probably true also for various organic dyes adsorbed onto TiO_2 . On the other hand, there is clear resonance Raman evidence [126] that $[\text{Fe}(\text{CN})_6]^{4-}$ forms a charge-transfer complex with TiO_2 . Accordingly, ultrafast (< 50 fs) electron photoinjection from $[\text{Fe}(\text{CN})_6]^{4-}$ has been attributed [122] to a direct $[\text{Fe}(\text{CN})_6]^{4-} \rightarrow \text{TiO}_2$ optical excitation. A full understanding of this problem would require a systematic investigation of the electron injection time and mechanism as a function of the anchoring group.

Whatever the detailed mechanism is, it is obvious that electron injection is much faster than any possible relaxation or redistribution of vibrational excitation energy in the excited sensitizer molecule. Hence, it takes place from vibrationally and/or electronically highly excited sensitizer molecules (Fig. 9). Apparently, the Marcus theory of electron transfer and its quantum versions cannot be applied here, since they assume equilibration of the donor molecule, that is of the excited sensitizer. Also, electronic interaction between a sensitizer donor and TiO_2 acceptor seems to be much stronger than is commonly assumed in these theories. It was suggested that the electron injection rate is controlled 'by the electron tunneling barrier, essentially determined by the anchor and spacer group, by the Franck–Condon overlap of the respective vibrational states of reactant and product, and by the escape time for the initially prepared wave packet describing the hot electron' [121]. Electronic coupling

through anchor groups (most often $-\text{COOH}$) facilitates electron transfer, since it provides electronic mixing between the bpy π^* orbital into which the electron is excited, and the ultimate TiO_2 acceptor orbitals [120]. The high density of acceptor

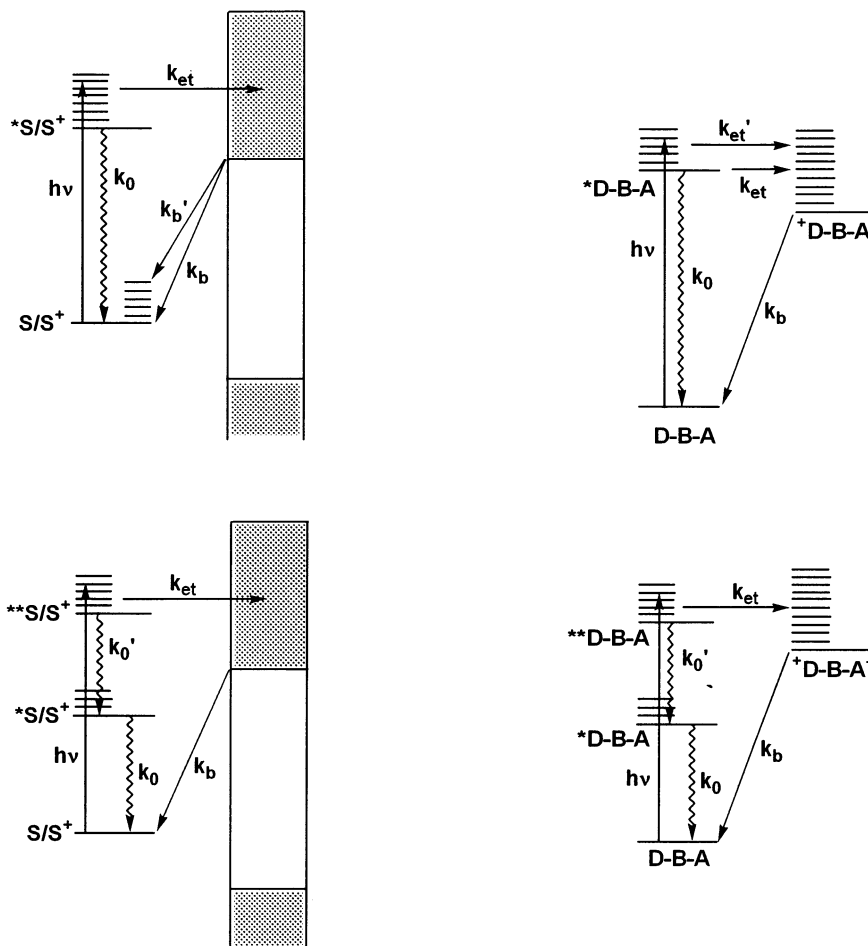


Fig. 9. Ultrafast electron transfer on a semiconductor electrode (left) and in supermolecular dyads (right). Upper left: electron injection from an excited sensitizer to a semiconductor electrode is ultrafast, taking place prior to or concurrently with vibrational relaxation, usually from a manifold of higher vibrational levels. Relaxation of the excited sensitizer to the ground state (k_0) is relatively unimportant, since $k_{et} \gg k_0$. Hence, even sensitizers with very short-lived excited states can be utilized. Two back-reactions are shown: a faster one (k_b) produces vibrationally-excited S^+ , slower one leads to relaxed S^+ (see text). Upper right: charge separation in a molecular dyad. Depending on the actual rate, the electron transfer can take place either from a vibrationally hot or relaxed $*D$. Bottom: capture of an upper electronic excited state ($**$) at a semiconductor electrode (left) or in a molecular dyad (right) will take place if $k_{et} \gg k_0'$. (The lower state $*S$ or $*D$ can lie either below (shown) or above the lower edge of the semiconductor conduction band or the $+D-B-A^-$ level, respectively. In the latter case, the electron transfer would occur from both states ($**$, and $*$) but, usually, with a different rate.

states in TiO_2 can be another reason for ultrafast injection rates [120]. More detailed quantitative theory is needed.

Femtosecond electron injection times also raise the question: from which electronic excited state of the sensitizer does the electron transfer actually occur? Typical injection times are definitely faster than the above mentioned 300 fs relaxation of the optically prepared $^1\text{MLCT}$ excited state of $[\text{Ru}(\text{bpy})_3]^{2+}$ to the $^3\text{MLCT}$ state [9]. The nature of the reactive state of the actual $[\text{Ru}(\text{bpy-4,4'-(COOH)}_2)_2(\text{NCS})_2]$ sensitizer is somewhat unclear. The relaxation time of the $^1\text{MLCT}$ state was determined as < 75 fs [120], only a little slower than the electron injection itself. Hence, it is possible that the electron transfer occurs, at least in part, directly from the $^1\text{MLCT}$ Franck–Condon excited state of the sensitizer, concurrently with its relaxation to the $^3\text{MLCT}$ state. The $^3\text{MLCT}$ state of $[\text{Ru}(\text{bpy-4,4'-(COOH)}_2)_2(\text{NCS})_2]$ has an inherent lifetime of 50 ns. However, it is dramatically shortened by attaching the sensitizer to the TiO_2 surface due to the ultrafast electron injection which renders the $^3\text{MLCT}$ state experimentally unobservable [95,120]. On the other hand, $[\text{Fe}(\text{bpy-4,4'-(COOH)}_2)_2(\text{CN})_2]$ provides a clear-cut example of a reaction from an upper excited state, since it was shown to inject an electron from its optically prepared $^1\text{MLCT}$ state [98]. The capture of higher excited states by ultrafast electron injection can improve the efficiency of light energy conversion, since only a little energy is wasted by thermal relaxation, see Fig. 9.

The overall efficiency of electron injection is limited by the dynamics of the injected electron in the semiconductor and by back electron transfer to the sensitizer cation (Fig. 9). These processes can also be ultrafast. Electron cooling in the TiO_2 conduction band takes place in less than 1 ps [120], while the back electron transfer dynamics are multiexponential: the main kinetic components spanning times from about 3 ps to as long as a few μs [95,120–122]. It is interesting to note that electron injection can leave the oxidized sensitizer (S^+) vibrationally excited. This can have important implications for initial stages of the back electron transfer: It was found that the back electron transfer in fluorescein-sensitized TiO_2 follows a highly non-exponential dynamics. It dramatically slows down within the first 30 ps, simultaneously with vibrational relaxation of the oxidized fluorescein dye [124,128]. This effect was explained by a driving force increase during vibrational relaxation of the oxidized dye cation (Fig. 9): since the back reaction occurs in the Marcus inverted region, the electron transfer rate slows down with increasing driving force, i.e. $k'_b > k_b$, see Fig. 9. This effect can be understood with the help of Fig. 11. (Note that in a complete solar cell, the electron is rapidly carried away from the surface of the semiconductor electrode and S^+ is regenerated by the mediator M^- , diminishing the importance of the back electron transfer for the cell efficiency.)

Electron injection from an excited sensitizer to a semiconductor electrode illustrates that an electron transfer reaction (τ_{et}) of an inherently long-lived (τ_0) molecular excited state can become ultrafast if the molecule is attached to a suitable electron acceptor. The excited-state lifetime (τ) is shortened accordingly: $1/\tau = 1/\tau_{\text{et}} + 1/\tau_0$. Even more interestingly, an extremely short-lived, upper molecular excited state can be captured and utilized by ultrafast electron injection that is faster than excited-state relaxation, see Fig. 9. In both cases, light energy is

harvested and virtually instantaneously converted to spatially separated electron and hole. This process can be very efficient because of its directionality, involvement of hot states, avoidance of photodecomposition of the photoactive molecule (sensitizer) and the huge difference between forward and back reaction rates. An extension of this principle to molecular systems, in which the semiconductor would be replaced by a molecular electron acceptor, could lead to supramolecular assemblies applicable in light energy conversion, photocatalysis, or molecular electronic devices [5,129]. Many coordination and organometallic compounds could find photochemical applications in this way, since even rapidly decaying excited states can be utilized. This can be accomplished in dyads of the type D-B-A, where D is a photo- and redox-active molecular fragment capable of excited-state electron transfer, A is an electron acceptor, and B is a covalent or hydrogen-bonded molecular bridge (molecular wire). Synthesis, characterization and photophysical studies of supramolecules comprised of linked excited-state electron donors and acceptors is a flourishing field of research. Various types of such photo-redox active supermolecules [5], that is chromophore–quencher complexes, dyads and more complicated triads, tetrads, dendrimers [130] etc., have been synthesized, often using very demanding procedures.

Indeed, photoinduced electron transfer from D to A:



is much faster in such assemblies, as compared with a bimolecular excited-state reaction of isolated molecules: ${}^*\text{D} + \text{A}$. This is well demonstrated by the following example [131]: The ca. 1 μs lifetime of the ${}^3\text{MLCT}$ excited state of $[\text{Ru}(\text{bpy})_3]^{2+}$ is shortened to a few tens of picoseconds when a methylviologen dication (MV^{2+}) is attached to the 4-position of the bpy ring by a $-(\text{CH}_2)_n-$ chain; $n = 1-8$. This is caused by a $\text{bpy}^{\bullet-} \rightarrow \text{MV}^{2+}$ intramolecular electron transfer, which occurs from the ${}^3\text{MLCT}$ excited state with a time constant of 17 ps or longer, depending on n . Very interesting ultrafast intramolecular redox reactions were also found [5,53,132–137] in supermolecules containing metalloporphyrin photo- and redox-active units.

In most of the dyads studied, the donor and acceptor units are separated by an organic spacer. The $[\text{Re}(\text{MQ}^+)(\text{CO})_3(\text{dmb})]^{2+}$ complex [138–140] represents a case where the two redox centers, dmb and MQ^+ , are linked only by a metal atom; $\text{MQ}^+ = N\text{-Me-4,4'-bipyridinium}$, $\text{dmb} = 4,4'\text{-Me}_2\text{-2,2'-bipyridyl}$. Optical excitation populates a $\text{Re} \rightarrow \text{dmb}$ MLCT excited state, which in the absence of oxidizing MQ^+ ligand, would have a lifetime of tens of nanoseconds [71]. However, the $\text{Re} \rightarrow \text{dmb}$ MLCT excited state $[\text{Re}^{\text{II}}(\text{MQ}^+)(\text{CO})_3(\text{dmb}^{\bullet-})]^{2+}$ undergoes an ultrafast intramolecular electron transfer $\text{dmb}^{\bullet-} \rightarrow \text{MQ}^+$ with a time constant of 8 or 14 ps in CH_3CN or ethylene glycol, respectively, see Fig. 10 [140]. This reaction converts the $\text{Re} \rightarrow \text{dmb}$ MLCT excited state to the $\text{Re} \rightarrow \text{MQ}^+$ MLCT state $[\text{Re}^{\text{II}}(\text{MQ}^*)(\text{CO})_3(\text{dmb})]^{2+}$, thus making a conceptual link between an electron transfer reaction and excited-state decay. Although the kinetics of this reaction can be accounted for by Marcus theory, it is well possible that the rate is actually controlled by conformational motion of the MQ^+ acceptor ligand, namely rotation around the interring C–C bond to attain planarity.

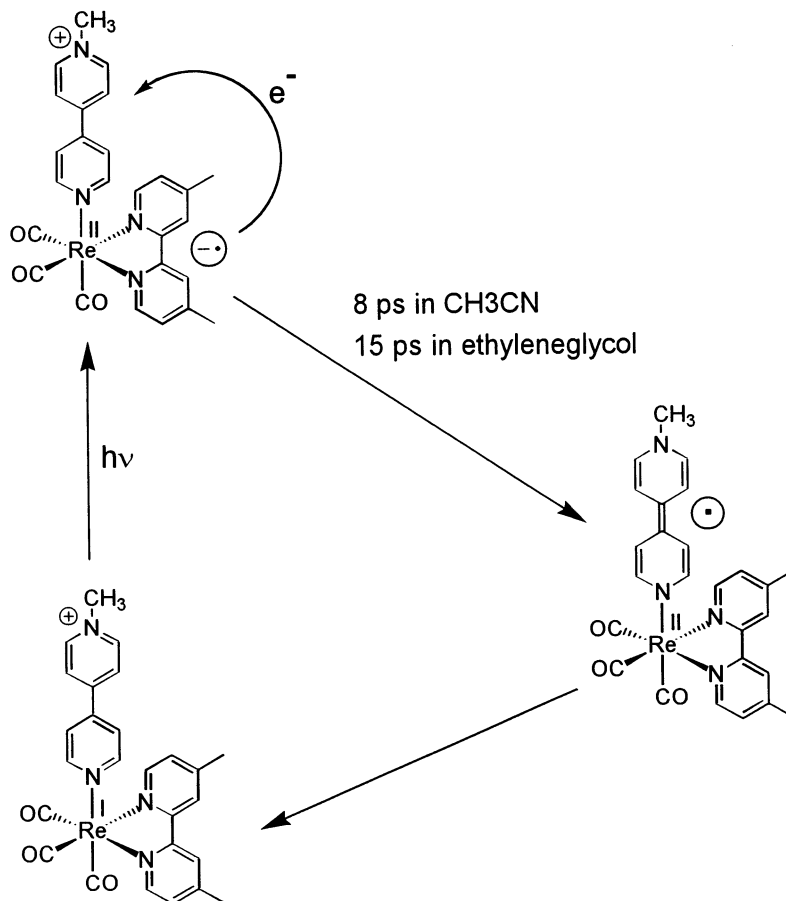


Fig. 10. Inter-ligand electron transfer from the $\text{Re} \rightarrow \text{dmb}$ MLCT excited state of $[\text{Re}(\text{MQ}^+)(\text{CO})_3(\text{dmb})]^{2+}$ [140].

Detailed kinetics of excited-state electron transfer in supramolecules are strongly dependent on the chemical nature, energetics (tunneling energy) and conformation of the bridging group B. Polyacetylene and poly-*p*-phenylene spacers seem to provide the fastest pathways, behaving as real molecular wires [81,82,141–143]. However, even the best molecular wires render the intramolecular electron (and energy) transfer in the picosecond range, well within the scope of traditional electron transfer theories which assume weak electronic coupling and thermal equilibration along reaction coordinate. Femtosecond intramolecular electron transfer, similar to that discussed above for sensitized semiconductors, is very rare in molecular dyads. It is quite possible that the difficulty of molecular systems in attaining femtosecond rates of intramolecular electron transfer is caused by an

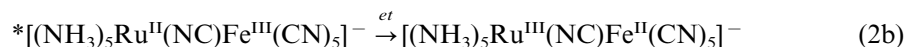
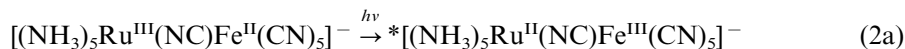
inherently much lower density of acceptor states and by weaker electronic coupling, as compared with semiconductors.

Nevertheless, there are molecular systems (dyads) in which it is possible to capture upper excited states by ultrafast electron transfer. This is the case of complexes of the type $[\text{Ir}_2(\mu\text{-pz})_2(\text{CO})_2(\text{PR}_2\text{-O-(CH}_2)_n\text{-py}^+)_2]^{2+}$ which contain a pyridinium electron acceptor covalently linked to the Ir_2 center through a phosphine ligand [40,41,43]. Electron transfer from an upper singlet state $^1\text{d}(\sigma^*)\text{p}(\sigma)$ of the Ir_2 unit to py^+ acceptor occurs in the picosecond time domain; 9–37 ps, depending on the bridge and the driving force. It is faster than the inherent 100 ps decay time of the $^1\text{d}(\sigma^*)\text{p}(\sigma)$ excited state in the absence of any electron acceptor. A truly ultrafast capture of an upper excited state has been observed in a $\text{Zn}(\text{porphyrin})\text{-Ru}(\text{bpy})_3$ dyad [133] and a $\text{Zn}(\text{porphyrin})^{4-} | \text{MV}^{2+}$ ion pair [144]. In both cases, optical excitation populates upper S_2 excited state of the $\text{Zn}(\text{porphyrin})$ unit which undergoes an electron transfer to $\text{Ru}(\text{bpy})_3^{3+}$ or MV^{2+} acceptors with time constants of 1.7 ps and ≤ 200 fs, respectively. Interestingly, the lower S_1 state of the $\text{Zn}(\text{porphyrin})\text{-Ru}(\text{bpy})_3^{3+}$ assembly reacts 100-times slower than the upper S_2 state. Such differences in reactivity of individual excited states of the same photoactive unit can be caused by a different driving force and electronic coupling. They can be utilized in ‘molecular devices where different electronic outputs are generated depending on the wavelength of the incident light’ [133]. The electron transfer rate observed for the S_2 state of $\text{Zn}(\text{porphyrin})^{4-} | \text{MV}^{2+}$ is one of the fastest known for a molecular system. Because of a very high driving force, this reaction occurs in the Marcus inverted region. The very fast rate has been attributed to the high density of acceptor states in the product, i.e. the reduced $\text{MV}^{\bullet+}$ radical-cation [144]. This allows the electron to be injected from the S_2 state of the $\text{Zn}(\text{porphyrin})$ unit into one of the upper product electronic states, making the reaction (nearly) activationless (Fig. 11).

Optical excitation of photoredox-active molecules in an electron-accepting solvent or in a very concentrated solution of an electron acceptor can trigger ultrafast electron transfer even if the redox partners are not bound together. The high acceptor concentration ensures close contact (encounter complex) with the photoactive species even at the instant of electronic excitation, overcoming kinetic limits imposed by diffusion. For example, the upper S_2 excited state of $\text{Zn}(\text{tetraphenylporphyrin})$ injects an electron into a CH_2Cl_2 solvent with a time constant of 1 ps [145]. This reaction is obviously similar to intramolecular electron transfer in $\text{Zn}(\text{porphyrin})^{4-} | \text{MV}^{2+}$ and $\text{Zn}(\text{porphyrin})\text{-Ru}(\text{bpy})_3^{3+}$ species discussed above. Femtosecond electron transfer has been observed between the excited oxazine dye and the *N,N*-dimethylaniline solvent [146,147] or ethylferrocene (2-molar) in acetonitrile [148]. The kinetics of the former reaction are highly nonexponential with principal time constants of 30 and 80 fs [149]. This behavior has been explained assuming a strong electronic coupling between the excited dye and the solvent that makes the electron transfer adiabatic. Hence, the rate is largely determined by nuclear dynamics. The fast kinetic component has been attributed [147] to electron transfer prior to the onset of energy dissipation, reflecting the initial vibrational motion of the excited oxazine dye/*N,N*-dimethylaniline encounter complex. The slow compo-

nent then corresponds to electron transfer with dissipation. Notably, rates of electron transfer from excited electron donors to acceptor solvents are very fast, approaching those found for electron injection from molecular sensitizers to semiconductors.

Another type of femtosecond electron transfer is represented by decay of intervalence charge transfer excited states, IVCT, of mixed-valence complexes [149–154]. This can be illustrated by $[(\text{NH}_3)_5\text{Ru}^{\text{III}}\text{NCFe}^{\text{II}}(\text{CN})_5]^-$ whose optical excitation (2a) prepares a $\text{Fe}(\text{II}) \rightarrow \text{Ru}(\text{III})$ IVCT excited state. Its decay (2b) is equivalent to a back electron transfer $\text{Ru}(\text{II}) \rightarrow \text{Fe}(\text{III})$:



Similar behavior has been found for analogous $[(\text{NH}_3)_5\text{M}^{\text{III}}(\text{NC})\text{M}^{\text{II}}(\text{CN})_5]^-$; $\text{M} = \text{Ru}, \text{Os}$ complexes. The back electron transfer (2b) is genuinely ultrafast. Its dynamics are strongly solvent-dependent. For example, the time constant of the $\text{Ru}(\text{II}) \rightarrow \text{Ru}(\text{III})$ back electron transfer in IVCT excited state $*[(\text{NH}_3)_5\text{Ru}^{\text{II}}(\text{NC})\text{Ru}^{\text{III}}(\text{CN})_5]^-$ ranges from about 90 fs in water or formamide to 300 fs in glycerol [152,153]. Obviously, back electron transfer of IVCT excited states of mixed valence complexes is much faster than forward electron transfer in photo-

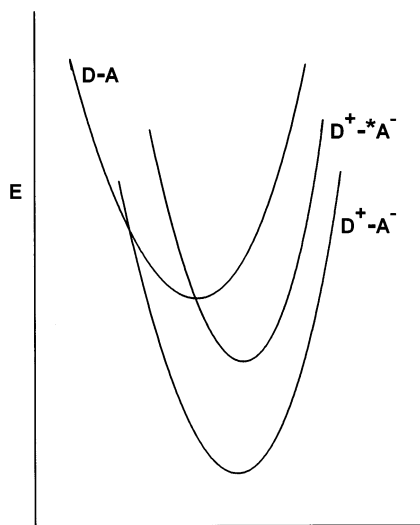


Fig. 11. Acceleration of an inverted electron transfer by formation of a low-lying excited state. Formation of the ground-state product D^+-A^- occurs in the Marcus inverted region with a considerable barrier. However, if the reduced acceptor (shown) or the oxidized donor possesses a low-lying excited state, the electron transfer can form this state with a lower or non-existent barrier (as shown). This phenomenon is responsible not only for the acceleration of an inverted electron transfer, but also for (electro)chemiluminescence [67] and for the absence of Marcus inverted behavior [44] in some highly energetic redox reactions.

redox-active dyads discussed above. Apparently, this is caused by stronger electronic coupling in mixed valence complexes, which renders the electron transfer partly adiabatic. Accordingly, the electron transfer rate is determined [152] by high-frequency nuclear motions and by the inertial solvent relaxation time. Hence, back electron transfer of IVCT excited states is faster in rapidly relaxing solvents like water or formamide [152]. Its rate is hardly temperature-dependent in these solvents, in accordance with activation of high-frequency promoting vibrations, presumably $\nu(\text{CN})$ stretches. Interestingly, the back electron transfer of IVCT states of mixed-valence complexes often produces a vibrationally excited electronic ground state. Its relaxation occurs as a follow-up process to the primary electron transfer. For example, the back electron transfer of the $\text{M(II)} \rightarrow \text{M(III)}$ IVCT state $*[(\text{NH}_3)_5\text{M}^{\text{II}}(\text{NC})\text{M}^{\text{III}}(\text{CN})_5]^-$; $\text{M} = \text{Ru}, \text{Os}$; produces vibrationally hot ground state of $[(\text{NH}_3)_5\text{M}^{\text{III}}(\text{NC})\text{M}^{\text{II}}(\text{CN})_5]^-$ in which the terminal $\nu(\text{CN})$ vibrations are excited up to seven vibrational quanta [151]. The vibrational relaxation takes place with time constants ranging from <0.5 to 6 ps for Ru and from 1.8 to 18 ps for Os, occurring much more slowly than the preceding electron transfer. As expected, higher vibrational levels decay faster than lower ones. Studies of back electron transfer reactions in mixed-valence complexes are very important for advancement of electron transfer theories. It is evident that the usual assumption of thermal equilibration of the reactive excited state is not always valid. The electron transfer reaction can proceed from several vibrational levels of the IVCT state, each of them representing a separate reaction channel. The vibrations coupled to the electron transfer remain activated in the product, effectively lowering the reaction barrier, since the electron transfer occurs in the Marcus inverted region (Fig. 11). Transfer of vibrational excitation to the product can also give rise to interesting coherence effects, which will be discussed below. They have been observed in $[(\text{NH}_3)_5\text{Ru}^{\text{III}}(\text{NC})\text{Fe}^{\text{II}}(\text{CN})_5]^-$; $\text{M} = \text{Ru}$ or Fe [153] and a polynuclear mixed valence complex Prussian blue [154]. Interestingly, it was also found that IVCT excitation induces magnetization of crystalline Prussian blue analogues [155]. The dynamics of this process were not studied.

Ultrafast back electron transfer also occurs from ion-pair charge transfer excited states, IPCT. An interesting example is provided [156] by the ion pair $\text{Cp}_2\text{V}^+ | \text{V}(\text{CO})_6^-$. Light irradiation excites simultaneously the IPCT electronic transition and the stretching CO vibration. Hence, optical excitation prepares a population of vibrationally hot IPCT excited states $\text{Cp}_2\text{V} | \text{V}(\text{CO})_6$. The IPCT excited state then undergoes back electron transfer, $\text{Cp}_2\text{V} \rightarrow \text{V}(\text{CO})_6$. Its rate is faster than vibrational relaxation and increases with increasing excitation of the $\nu(\text{CO})$ vibration in the IPCT state. Thus, the electron transfer from the $v = 2$ level of the IPCT state to the $v = 3$ level of the ground-state ion pair takes place with a time constant of 5.5 ps. Lower levels react more slowly as time constants of 11.3 and 26.4 ps were observed [156] for $v = 1 \rightarrow v = 2$ and $v = 0 \rightarrow v = 1$ electron transfers, respectively. This experiment clearly demonstrates that individual vibrational levels of CT excited states can provide separate reactivity channels with distinct dynamics. This conclusion is relevant also for back reactions of IVCT states of mixed-valence complexes, as was discussed above.

4.3. Intramolecular energy transfer

Intramolecular energy transfer is another ultrafast process available to supramolecular assemblies of chromophoric molecules [5,142,143,157–159]. This is especially the case of supermolecules which combine $\text{Ru}^{\text{II}}(\text{polypyridyl})_n$ and $\text{Os}^{\text{II}}(\text{polypyridyl})_n$ units linked by suitable bridging groups, namely acetylenes and phenylenes. Energy transfer is directed to Os centers whose MLCT excited states are lower in energy. Supermolecules consisting of porphyrins and/or metalloporphyrins also readily undergo efficient, ultrafast (ps) intramolecular energy transfer [160–163]. This is a very important natural phenomenon whereby light energy, absorbed by chromophore assemblies in plant photosynthetic centers, is transferred, in the form of electronic excitation energy, to the reactive chlorophyll special pair. Such ‘antenna systems’ composed of many chromophores allow the harvesting of light energy to occur with high efficiency. In molecular devices, an ultrafast, vectorial energy transfer can provide an alternative to electron transfer in information storage and manipulation.

Although many supermolecules exhibiting ultrafast energy transfer have been synthesized and their photophysics investigated, little attention has been paid to the understanding of the factors that control energy transfer rate. Intramolecular energy transfer usually occurs by the Dexter mechanism which is conceptually similar to intramolecular electron transfer [164–166]. It is based on through-bond electron exchange. It can also be viewed as a simultaneous electron and hole transfer through the LUMO and HOMO orbitals, respectively, of the bridging group. Hence, the energy transfer rate is strongly dependent on the nature of the bridging group connecting the initially excited chromophore and the ultimate excitation-energy acceptor. For example, supermolecules composed of $\text{Ru}(\text{bpy})_3^{2+}$ and $\text{Os}(\text{bpy})_3^{2+}$ units whose bpy ligands are connected by a $-\text{C}\equiv\text{C}-$ group undergo $\text{Ru} \rightarrow \text{Os}$ energy transfer on a time scale of a few picoseconds [167]. The actual rate is only slightly dependent on the positions through which the bpy ligands of the Ru and Os units are connected, but it increases with decreasing energy gap between triplet excited states of the donor and the bridge. This finding indicates the possibility of optimizing and controlling intramolecular energy transfer by structural modifications of the bridge structure.

The proper choice of the right bridging unit can also discriminate between energy and electron transfer in supermolecules capable of both. The $\text{Zn}(\text{porphyrin})-\text{Ru}(\text{bpy})_3^{2+}$ dyad provides a good example [168]. If the two active units are linked by a $-p\text{-C}_6\text{H}_4\text{-NH-C(O)-}$ group, an ultrafast electron transfer from the upper S_2 state of $\text{Zn}(\text{porphyrin})$ to the $\text{Ru}(\text{bpy})_3^{2+}$ unit occurs [133], as was discussed above. However, a similar dyad which uses a *trans* $-\text{C}\equiv\text{C}-\text{Pt}(\text{P}^n\text{Bu}_3)_2-\text{C}\equiv\text{C}-$ bridge shows an ultrafast $\text{S}_2 \rightarrow \text{Ru}(\text{bpy})_3^{2+}$ energy transfer (time constant ca. 3 ps), but no electron transfer. An interesting example of discrimination between picosecond energy and electron transfer from an excited $\text{Ru}^{\text{II}}(\text{trpy})$ terminus to the $\text{M}(\text{trpy})_2$ central unit by the choice of the metal atom M (Fe(II) or Co(II), respectively) is provided [141] by $[(\text{trpy})\text{Ru}(\text{trpy}-(\text{C}\equiv\text{C})_n-\text{trpy})\text{M}(\text{trpy}-(\text{C}\equiv\text{C})_n-\text{trpy})\text{Ru}(\text{trpy})]$ triads; $n = 1, 2$. Energy transfer occurs for

M = Fe(II) whereas the M = Co(II) center is oxidized to Co(III) by a $\text{Co(II)} \rightarrow {}^*\text{Ru}^{\text{II}}(\text{trpy})$ excited-state electron transfer.

Intriguing energy transfer behavior is exhibited [166] by the $[(\text{H}_2\text{-porphyrin-trpy})\text{Ru}(\text{trpy-porphyrin-Au})]$ triad with directly linked components. Optical excitation of the $\text{Ru}(\text{trpy})_2$ chromophore is followed by an ultrafast (< 20 ps) energy transfer from its ${}^3\text{MLCT}$ state to either of the peripheral porphyrin units, producing $[(\text{H}_2\text{-*porphyrin-trpy})\text{Ru}(\text{trpy-porphyrin-Au})]$ and $[(\text{H}_2\text{-porphyrin-trpy})\text{Ru}(\text{trpy-*porphyrin-Au})]$. Secondary energy transfer ($\text{Au-*porphyrin} \rightarrow \text{H}_2\text{-*porphyrin}$) in the latter species is about 2000-times slower (40 ns). It is a long-distance, through-bond process, mediated by the, now ground state, $\text{Ru}(\text{trpy})_2$ central unit.

4.4. Ultrafast bond splitting

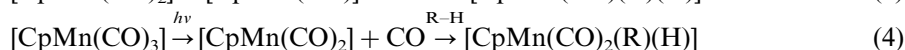
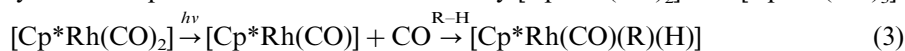
Splitting of a covalent bond is a fundamental chemical process. It can proceed very rapidly, provided that optical excitation prepares an unbound excited state. Earliest chemical applications of femtosecond spectroscopy concerned photochemical bond splitting in simple gas-phase molecules like I_2 , ICN , HgI_2 , NaI or NaCl [169,170]. The dissociation time of an I-CN bond was measured as 205 fs. Detailed investigations of I-I bond homolysis in an I_2 molecule brought further insight to the chemical physics of bond splitting and effects of the medium (gas phase, rare-gas atom clusters, solutions, host-guest complexes). A wealth of mechanistic information was also obtained [171] by femtosecond studies of HgI_2 in solution.

Electronic excitation of transition metal organometallic complexes often results in ultrafast metal–ligand bond splitting. Occurring either as a ligand dissociation or homolysis, photochemical bond splitting produces coordinatively unsaturated Lewis acidic metal fragments or radicals, respectively. Besides their fundamental importance, these photochemical reactions rapidly generate active catalysts or photoinitiators. A detailed understanding of excited-state bond splitting in organometallic compounds is very desirable, since it can test fundamental bonding theories and reveal relationships between the molecular structure and nature of excited states, their early dynamics, and overall photoreactivity.

Photochemical dissociation of a CO ligand from group 6 hexacarbonyls is a prototypical reaction whose studies on still shorter time scales have closely followed every technical advance in time-resolved spectroscopy. According to the latest seminal results [172], dissociation of a CO ligand from $\text{M}(\text{CO})_6$; $\text{M} = \text{Cr}, \text{Mo}, \text{W}$; is really ultrafast, being completed in a time interval shorter than 240 fs after excitation. The photoproduct, naked $\text{M}(\text{CO})_5$ species, is formed vibrationally excited and its cooling, including solvation, has a time constant of about 22 ps. Geminate recombination of photoproducts still trapped in the solvent cage occurs with a time constant of ca. 150 fs. It produces vibrationally hot $\text{M}(\text{CO})_6$ which cools with time constants of 112 ps ($\text{M} = \text{Cr}$) or 70 ps ($\text{M} = \text{Mo}, \text{W}$). This study has clearly shown that photochemical ligand dissociation can occur on a time scale much faster than vibrational relaxation, presumably directly from an optically prepared Franck–Condon excited state. The reactive state has long been assumed

to be LF, originating in $t_{2g} \rightarrow e_g$ excitation. However, recent DFT and TD-DFT computational studies [173–175] have suggested that low-lying excited states of $\text{Cr}(\text{CO})_6$ have a $\text{Cr} \rightarrow \text{CO}$ MLCT character. Moreover, calculations revealed that the corresponding potential energy curves are unbound along the $\text{Cr}-\text{CO}$ coordinate. Hence, it appears that CO dissociation from $\text{Cr}(\text{CO})_6$ actually occurs from a MLCT state.

Ultrafast CO dissociation has been observed for $[\text{Rh}(\text{CO})_2(\text{acetylacetonate})]$ [111], and for carbonyl complexes which photochemically activate [176–182] C–H bonds in hydrocarbons or Si–H bonds in silanes: $[\text{Cp}^*\text{M}(\text{CO})_2]$; $\text{M} = \text{Rh}, \text{Ir}$; [111,183,184], $[\text{Tp}^*\text{Rh}(\text{CO})_2]$; $\text{Tp}^* = \text{HB}(3,5\text{-Me}_2\text{-pyrazolyl})_3$ [182,185,186], or $[\text{CpM}(\text{CO})_3]$; $\text{M} = \text{Mn}, \text{Re}$; [182,187,188]. A CO ligand dissociates from these complexes on a femtosecond time scale, apparently directly from a Franck–Condon excited state. The nature of the reactive excited state has not been studied. Although a traditional explanation of organometallic photochemistry [21] would imply a metal-centered excited state, a strong contribution of a $\text{M} \rightarrow \text{CO}$ MLCT character may well be assumed. Photogenerated CO-loss products undergo oxidative addition reactions with hydrocarbons or silanes (RH) to form alkyl-hydrido or silyl-hydrido complexes. This is demonstrated by $[\text{Cp}^*\text{Rh}(\text{CO})_2]$ and $[\text{CpMn}(\text{CO})_3]$:

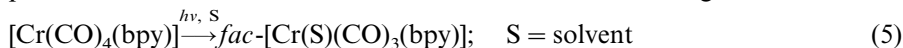


$\text{R} - \text{H} = \text{hydrocarbon/silane}$

For $[\text{Cp}^*\text{M}(\text{CO})_2]$, it has been shown [183] that the quantum yield of CO dissociation is limited by branching of evolution of the excited-state population between CO dissociation and relaxation into lower-lying unreactive excited states, which decay to the ground state in 30–40 ps. Most of the experimental effort has been devoted to the elucidation of the mechanisms and kinetics of subsequent reactions between CO-loss primary photoproducts and hydrocarbon or silane substrates. These reactions can proceed through several channels, involving direct substrate coordination, dechelation of a Tp^* ligand, or a Cp^* ligand hapticity change. Substrate coordination is itself ultrafast, taking place on a picosecond time scale, apparently alongside the vibrational relaxation of primary photoproducts. It precedes the oxidative addition proper. Et_3SiH can coordinate to photoproducted CO-loss species by its Si–H end or by an Et substituent. These two modes of coordination open two different reaction channels. An ultrafast rate of 4.4 ps has been determined [188] for Si–H bond splitting upon coordination of Et_3SiH to photogenerated $[\text{CpRe}(\text{CO})]$. Interestingly, the essential features of this photochemical C–H or Si–H bond activation, including dechelation of a Tp^* ligand, have originally been deduced [176–181] from detailed studies of photochemical quantum yields as a function of reaction conditions. The ultrafast studies discussed above provided kinetic data, confirmed the identity of intermediates involved and revealed further mechanistic details [182].

Ultrafast CO dissociation has also been found for carbonyl-diimine complexes, especially of 1st row transition metals. These reactions are interesting mechanisti-

cally [189,190], since irradiation excites the metal \rightarrow diimine MLCT transition, which does not involve orbitals that are strongly bonding or antibonding with respect to a metal–CO bond. Hence, it is important to determine whether the optically populated MLCT state is the reactive state proper and, if so, what makes it dissociative. Photochemistry of $[\text{Cr}(\text{CO})_4(\text{bpy})]$ has been much studied [100,191–196] as a prototypical reaction of this type. Irradiation into the lowest MLCT absorption band leads to ultrafast dissociation of an axial CO ligand:



A femtosecond spectroscopic study [100] has revealed that the $[\text{Cr}(\text{S})(\text{CO})_3(\text{bpy})]$ photoproduct is formed within 400 fs after excitation, alongside relaxation into two lower-lying unreactive excited states, presumably $^3\text{MLCT}$. The latter two states then decay to the ground state with lifetimes of 8 and 87 ps, respectively. Moreover, it was found [100] that the relative branching ratio between the reactive and relaxation pathway decreases with decreasing excitation energy across the spectral region of the MLCT absorption band in the same way as the overall quantum yield [195], measured with continuous irradiation. The reactive state obviously keeps a memory of initial excitation. This rules out an occurrence of any relaxation (thermalization) between the optical excitation and reaction. Hence, it can be concluded that CO dissociation and electronic relaxation are concurrent ultrafast processes which take place directly from the optically prepared Franck–Condon $^1\text{MLCT}$ state. Branching ratio between reactive and relaxation channels determines the photochemical quantum yield. The $[\text{Cr}(\text{CO})_4(\text{bpy})]$ example well demonstrates how the overall photochemistry is determined by the initial excited-state dynamics that occur within few tens or, at most, hundreds of femtoseconds. The high reactivity of the $^1\text{MLCT}$ state of $[\text{Cr}(\text{CO})_4(\text{bpy})]$ and analogous complexes has been explained [189,197,198] by an interaction between the MLCT state and an upper LF state that occurs along the Cr–CO reaction coordinate and renders the potential energy curve of the MLCT state nearly unbound, with only a small barrier, that is manifested [195] by a quantum yield temperature-dependence.

Dissociative isomerization of $[\text{Mn}(\text{Br})(\text{CO})_3(^i\text{Pr-DAB})]$; $^i\text{Pr-DAB} = ^i\text{Pr-N}=\text{CH-CH}=\text{N-}^i\text{Pr}$; represent another type of photochemical CO dissociation [199–201], see Fig. 12. Optical excitation prepares an excited state of a mixed ($\text{Mn} \rightarrow \text{DAB MLCT}/(\text{Br} \rightarrow \text{DAB LLCT})$ character (LLCT = ligand-to-ligand charge transfer) [200,202]. Dissociation of an equatorial CO ligand follows [203] with a time constant of 11 ps. According to theoretical prediction [202], it is accompanied by a movement of the axial Br ligand toward the vacated equatorial site (Fig. 12). The relatively slow rate of CO dissociation from $[\text{Mn}(\text{Br})(\text{CO})_3(^i\text{Pr-DAB})]$ is in a stark contrast to the femtosecond rates found for $\text{Cr}(\text{CO})_6$, $[\text{Cr}(\text{CO})_4(\text{bpy})]$ and other carbonyls discussed above. This ca. 50-fold difference in reaction rate seems to be caused by the different potential energy curve shapes of the respective reactive excited states along the M–CO reaction coordinate. Whereas quantum chemical calculations on $\text{Cr}(\text{CO})_6$ [174] and $[\text{Cr}(\text{CO})_4(\text{bpy})]$ [198], point to unbound shapes, all excited states calculated [202] for the model complex $[\text{Mn}(\text{Cl})(\text{CO})_3(\text{H-DAB})]$ show a deep minimum along both axial and equatorial Mn–CO coordinates.

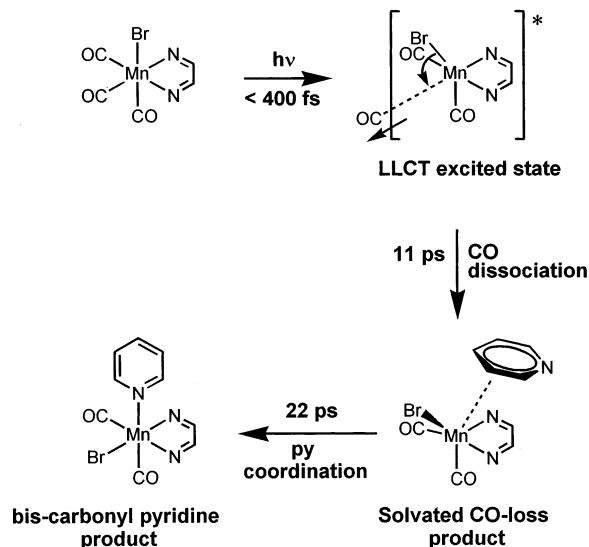


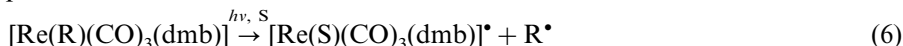
Fig. 12. Dynamics of photochemical dissociative isomerization of $[\text{Mn}(\text{Br})(\text{CO})_3(\text{Pr-DAB})]$.

However, the excited-state potential energy curve for equatorial CO dissociation is immersed in the energy well formed by a ground state potential energy curve. Under such conditions, CO dissociation can occur by resonantly-enhanced coupling between the electronically excited state and the ground state dissociation continuum that exists above the energy barrier for a ground state CO dissociation [202]. Such a coupling allows CO dissociation to occur, but much more slowly than if following a dissociative potential energy surface.

An interesting case of dual ultrafast photoreactivity is represented by $\text{Mn}_2(\text{CO})_{10}$. Its excitation results in simultaneous axial CO dissociation and Mn–Mn bond homolysis [204–207]. The relative importance of these reactions depends on excitation energy, with CO dissociation dominating under high-energy UV excitation. CO dissociation initially produces $\text{Mn}_2(\text{CO})_9$ with terminal CO ligands. Within about 20 ps, it rearranges into $(\text{CO})_4\text{Mn}(\mu\text{-CO})\text{Mn}(\text{CO})_4$. A gas phase femtosecond study [207] has shown that both CO dissociation and Mn–Mn homolysis are femtosecond processes which occur with time constants of 20 and 40 fs, respectively. These extreme rates clearly point to the unbound character of the reactive excited states responsible. Optical excitation prepares $^1\sigma\sigma^*$ and $^1d_\pi\sigma^*$ excited states in a ratio which depends on the excitation wavelength used. A quantum chemical (DFT) study has identified [208] the state responsible for Mn–Mn homolysis as $^3\sigma\sigma^*$ while the $^1d_\pi\sigma^*$ (or $^3d_\pi\sigma^*$) state is responsible for CO dissociation, the σ and σ^* labels being pertinent to the Mn–Mn bond. Indeed, calculations have confirmed the unbound character of these states with respect to the relevant reaction coordinates. At first glance, it is not obvious why population of a $d_\pi\sigma^*$ state should lead to

prompt CO dissociation. Calculations have shown that it is caused by an admixture of an axial Mn–CO antibonding orbital to the $d_{\pi}\sigma^*$ state, that occurs along the reaction coordinate.

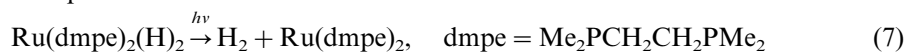
Dynamics of ultrafast photochemical metal–alkyl bond homolysis has been studied [62,63] in some detail using the organometallic carbonyl-diimine complexes $[\text{Re}(\text{R})(\text{CO})_3(\text{dmb})]$; R = Me, Et, dmb = 4,4'-Me₂-2,2'-bipyridyl; as prototypical examples:



Re–R bond homolysis occurs from a triplet sigma bond to ligand charge transfer, ³SBLCT, excited state. This excited state originates [25,209] in electron excitation from an orbital that is σ -bonding with respect to the Re–R bond into a π^* orbital of the dmb ligand. (Hence, SBLCT states are often denoted $\sigma\pi^*$.) Optical excitation of either complex prepares a mixed ¹MLCT/SBLCT excited state which evolves along two channels: (i) direct Re–R bond homolysis via a dissociative ³SBLCT state, and (ii) population of an unreactive excited state of a ³MLCT/SBLCT character. For $[\text{Re}(\text{Me})(\text{CO})_3(\text{dmb})]$, ³MLCT/SBLCT is the lowest excited state and its population prevents any further reactivity. It is a true trapping state, which decays to the ground state with a lifetime of 35–40 ns. Branching of the Franck–Condon excited-state evolution, that is a simultaneous formation of radical products and population of the trapping state, is completed within 400 fs after excitation [63]. The corresponding branching ratio and, hence, the photochemical quantum yield are dependent on temperature, indicating a barrier on the reaction pathway [62]. This barrier arises from the interaction between the Franck–Condon ¹MLCT/SBLCT and ^{1,3}SBLCT states along the reaction coordinate. The situation is different for $[\text{Re}(\text{Et})(\text{CO})_3(\text{dmb})]$, since its reactive ³SBLCT state is the lowest excited state everywhere along the reaction coordinate. The time constant of the branching between the direct Re–Et homolysis and population of the unreactive ³MLCT/SBLCT state was estimated [63] as 600–800 fs. However, the ³MLCT/SBLCT state now lies above the reactive ³SBLCT state, through which it reacts to the radicals. Population of the unreactive ³MLCT/SBLCT state thus provides a second, delayed ($\tau \cong 200$ ps in CH₂Cl₂) pathway for Re–Et bond homolysis [63]. The excited-state dynamics of $[\text{Re}(\text{R})(\text{CO})_3(\text{dmb})]$; R = Me, Et; complexes are schematically compared in Fig. 13.

Optical excitation of axially-coordinated metalloporphyrins, including biologically relevant heme proteins, triggers an ultrafast dissociation of the axial ligand: O₂, CO, or NO. The metalloporphyrin is produced vibrationally excited. Hence, these reactions are used to investigate metalloporphyrin or metalloprotein vibrational dynamics by femto/picosecond time-resolved spectroscopic techniques [107,108,116,117,210,211]. An ingenious use of picosecond time-resolved polarized IR spectroscopy has even revealed [212] the relative orientations of the CO ligand with respect to the heme plane of carbonylmyoglobin before and after CO photodissociation. The large reorientation observed accounts for the inefficient recombination and also explains how myoglobin discriminates between O₂ and toxic CO.

Photochemical reductive eliminations are also typical ultrafast reactions. For example, it has been shown [213,214] that Ru–H bond cleavage, H–H bond formation and rearrangement of $[\text{Ru}(\text{bis-phosphine})_2]$ product are fully completed within 16 ps:



Examples of ultrafast photochemical metal–ligand bond homolysis discussed in previous paragraphs show that it is not possible to interpret organometallic photoreactivity using only the excited state orbital parentage at the geometry of vertical (Franck–Condon) excitation. Instead, energies, characters, and interactions

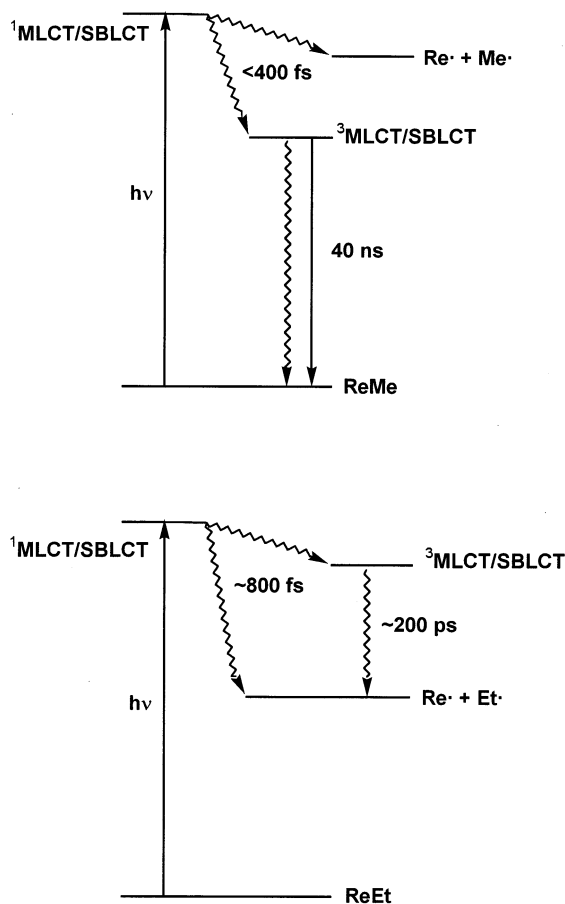


Fig. 13. Excited-state dynamics and photochemistry of $[\text{Re}(\text{R})(\text{CO})_3(\text{dmb})]$; $\text{R} = \text{Me}, \text{Et}$ [63]. $^1\text{MLCT}/\text{SBLCT}$ is the optically prepared Franck–Condon state. Radical formation actually involves an intersystem crossing and mixing with the reactive $^3\text{SBLCT}/\text{MLCT}$ state along the reaction coordinate. (The excited states involved have a heavily mixed character due to a mixing between Re–R σ and dmb π^* orbitals [248]. The SBLCT character predominates in $^3\text{SBLCT}/\text{MLCT}$.)

(mixing) of all relevant excited states along possible reaction coordinates must be considered [99]. This is best accomplished by advanced quantum chemical calculations which yield reliable potential energy curves of ground as well as excited states. Very interesting results, which can be directly used for photochemical interpretation, have been obtained from CASSCF calculations, for example, on $[\text{HCo}(\text{CO})_4]$ [215,216], $[\text{H}_2\text{Fe}(\text{CO})_4]$ [217], several $[\text{M}(\text{R})(\text{CO})_3(\text{H-DAB})]$ complexes; $\text{M} = \text{Mn}$ or Re , $\text{R} = \text{H}$, Me , Et ; [218–222], and $[\text{Cr}(\text{CO})_4(\text{bpy})]$ [198]. Subsequent wave packet propagations on calculated potential energy surfaces afford information on branching of the Franck–Condon state evolution between various reaction and/or relaxation channels, yields and dynamics of ultrafast processes. Some interesting predictions, still to be tested experimentally, have been made about effects of excitation energy and additional vibrational excitation. For $[\text{HCo}(\text{CO})_4]$ and $[\text{M}(\text{H})(\text{CO})_3(\text{H-DAB})]$, it was even possible to simulate intersystem crossing between spin-singlet and triplet excited states [222,223]. This work in theoretical organometallic photochemistry has been the subject of several reviews [224–227]. Density functional theory, DFT, has also been applied to photochemical problems, although its validity in calculating higher excited states is not rigorously proven. Nevertheless, it has been successfully used to calculate potential energy curves describing CO photodissociation from $\text{Cr}(\text{CO})_6$ [174], both Mn–Mn bond homolysis and CO dissociation from $\text{Mn}_2(\text{CO})_{10}$ [208], dissociative isomerization of *fac*- $[\text{Mn}(\text{Cl})(\text{CO})_3(\text{H-DAB})]$ [202], and to explain different photoreactivity of *fac*- and *mer*-isomers of $[\text{Mn}(\text{Cl})(\text{CO})_3(\text{H-DAB})]$ [228]. This work was reviewed in reference [173]. Further progress in the theoretical understanding of organometallic photochemical reactions, especially of those involving charge-transfer states will require to include solvent effects. First steps in this direction are being made [229].

4.5. Coherent phenomena

Of the several types of coherence [3] which can be generated by optical excitation with femtosecond light pulses, vibrational coherence is photochemically the most interesting. In brief, vibrational coherence is initially generated on the potential energy surface of the optically prepared excited state as a superposition of several vibrational eigenstates whose phases and amplitudes are related. It concerns only those vibrational modes which are activated by optical excitation, that is vibrations along those normal coordinates which are displaced on excitation. Excitation of an ensemble of molecules by a light pulse whose duration is shorter than molecular vibrational motion creates a collective coherence, whereby all the excited molecules vibrate in phase. Ensemble dynamics thus reflect the dynamical behavior of constituent molecules. Provided that the Franck–Condon state undergoes a chemical reaction or electronic relaxation that is faster than relaxation and redistribution of vibrational energy, a vibrational coherence can persist through the course of the reaction and is transferred to the product. Besides that, coherent movements may also arise from vibrations activated by the ultrafast excited-state reaction proper. Vibrational coherence is manifested in time-resolved spectra by damped oscillations on transient-signals time-profiles. In solutions, these oscillations can persist for as

long as 1–2 ps. Their Fourier transformation yields frequencies and phases of the relevant vibrations while damping is equal to the vibrational dephasing time. An observation of a vibrational coherence in a product shows that it is formed directly (diabatically) by a reaction occurring on the potential energy surface of a Franck–Condon excited state, without much relaxation along the reaction coordinate. Detailed analysis of vibrational coherence affords valuable information on the role of specific vibrational motions in promoting excited-state reactions and on the coupling to solvent or, in the case of supramolecules or metalloproteins, to vibrations of surrounding molecular matrix. These studies are attractive even from the point of view of conventional photochemistry since information obtained is pertinent to behavior of individual molecules, even under continuous irradiation or long-pulse experiments which, of course, do not induce any ensemble coherence [3].

Many of the photochemical processes discussed in previous sections lead to vibrationally excited products. In fact, this is a commonplace phenomenon for ultrafast photochemical reactions. Provided that the conditions discussed in the preceding paragraph are met, vibrational coherence in the product state can be observed. For example, prominent oscillations due to the $\nu(\text{HgI})$ vibration in HgI photoproduct were observed [171] upon 38 fs excitation of HgI_2 in ethanol. Analysis of coherences obtained after NO photodissociation from nitrosyl-myoglobin (MbNO) has revealed [117] that NO dissociation occurs in less than 75 fs, being followed by rapid compression of the Fe–histidine bond. It also triggers a doming motion of the heme unit. These two vibrational motions occur with periods of 148 fs and 428 fs, respectively. It is interesting to note that the Fe–histidine mode is not active in resonance Raman spectrum of MbNO , i.e. that the Fe–histidine bond is not affected by the Franck–Condon electronic excitation. Hence, the coherent Fe–histidine and doming motions observed in the Mb photoproduct represent a response of the heme moiety to NO dissociation. Observation of a vibrational coherence is especially important for electron transfer reactions since it allows the identification of promoting vibrations. Unlike resonance Raman spectroscopy, coherence studies can, in principle, determine both the relevant excited state nuclear displacements and electron transfer dynamics at identical conditions, using the same experiment. For example, coherent vibrations of oxazine-1 radical observed [147] after its formation by a 30–80 fs electron transfer between oxazine-1 cation and *N,N*-dimethylaniline solvent point to the high importance of nuclear motions, typical for an adiabatic reaction. Vibrational coherence observed [153] in the product state $[(\text{NH}_3)_5\text{Ru}^{\text{III}}(\text{NC})\text{Fe}^{\text{II}}(\text{CN})_5]^-$; $\text{M} = \text{Ru}$ or Fe ; formed by a back electron transfer of an IVCT state (reaction (2b)) is due to vibrations activated by Franck–Condon excitation. The dephasing time is very fast, 300 fs, but still slower than electron transfer, ca. 90 fs. Hence, some vibrational coherence is maintained through the back electron transfer. However, it is not clear if/how this vibrational coherence affects the electron transfer kinetics proper. Vibrational coherence that dephases on a time scale comparable with that of electron transfer has also been found [154] upon IVCT excited-state decay of a polynuclear mixed valence complex Prussian blue.

Another interesting example is provided by blue copper proteins [118]. Their Cu-localized LF excited state relaxes with a time-constant of 200–300 fs, depending on the actual protein. Vibrational coherence is transferred to the recovered ground state. It corresponds to a combination of several skeletal vibrations, the Fe–S(cysteine) stretch being most prominent, and to motions of the protein surroundings of the Cu center. The dephasing time is 0.56–2.5 ps, depending on the vibration. This shows that the large structural reorganization around the Cu-center, caused by LF electronic excitation, is carried through relaxation to the ground state, affecting also protein surroundings. Moreover, this system also shows an additional short-lived vibrational coherence, specific to the LF excited state.

Electronic coherence decays much more rapidly than vibrational coherence. It is experimentally manifested in time-resolved absorption spectroscopy by an intense signal (spike) at zero time delay, observed with parallel polarization of excitation and probe laser pulses. This effect has been detected for mixed-valence complexes $[(\text{NH}_3)_5\text{Ru}^{\text{III}}(\text{NC})\text{Fe}^{\text{II}}(\text{CN})_5]^-$; $\text{M} = \text{Ru}$ or Fe ; [153] and Prussian blue [154]. However, in these cases, the electronic coherence decays within about 20 fs, that is faster than the back electron transfer in corresponding IVCT states. Effects of electronic coherence on photochemical reactions have not yet been demonstrated.

5. Ultrafast, fast, or slow photoprocesses: challenges and perspectives

Based on their dynamics, two broad types of photochemical processes emerge: (i) ultrafast, which occur on a time scale comparable with that of vibrational or even electronic motion in the active chromophore and its surroundings, and (ii) relatively slow reactions of relaxed, thermally equilibrated excited states. Processes occurring on different photochemical time scales are closely interrelated, since every reaction of a relaxed excited state is preceded by ultrafast relaxation steps. This can be relevant to potential applications since light energy or information can be captured by an ultrafast electron- or energy-transfer and stored as a resultant long-lived charge-separated or excited state. Or, vice versa, reactions of otherwise long-lived excited states can be accelerated into the ultrafast regime by incorporating respective chromophores into properly designed supermolecules or attaching them to a semiconductor surface.

Mechanistically, ultrafast reactions are still little understood. From an experimental point of view, investigations of ultrafast photoprocesses amount to a chemist's race against time: it is an attempt to see the fastest chemically relevant molecular changes and transformations. Technically, with laser pulses only a few tens of femtoseconds long readily available, we are now near the end of this race. However, the necessary state-of-the-art instrumentation and specific expertise are available only in a few specialized laboratories. So far, too few chemically interesting systems have been studied to map possible ultrafast phenomena and draw general conclusions. Hence, systematic explorations of ultrafast photochemical dynamics of coordination and organometallic compounds are very important and will certainly continue. The vast number of interesting photochemical reactions

reported in the literature [5,23,230] provides much inspiration. Both small, mononuclear complexes with relatively simple ligands and large, complicated supermolecules provide a challenge. Studies on simple molecules, whose electronic and vibrational transitions can be properly assigned, will provide the much needed detailed physico-chemical understanding of early excited-state dynamics. Real-time studies of intramolecular electron transfer, metal–ligand and intraligand bond-splitting, ligand association, isomerization, etc., and of their underlying excited-state dynamics are very promising. The dynamic role of the solvent (medium), assessment of the degree of adiabaticity and of the role of specific intramolecular vibrations in these reactions are very important questions. Achieving a physically correct explanation of experimentally observed temperature and pressure effects on yields of ultrafast reactions is another challenge. The examples discussed above stress the need for close interplay between ultrafast experimental studies and quantum-chemical calculations of potential energy surfaces, wave packet propagation and modeling of solvent effects. It is expected that detailed understanding of ultrafast dynamics of well-chosen archetypal complexes and reactions will allow the formulation of general rules and principles, qualitatively applicable throughout coordination and organometallic photochemistry. Unravelling the relations between the ground state structure, nature of low-lying excited states, their early dynamics and overall photochemistry is an important part of this research. A coordinated experimental and theoretical research would thus help both to understand photochemical mechanisms and to test fundamental theories of chemical bonding and solvation.

Investigations of large systems, especially supermolecules, will address these and additional questions and, potentially, unravel new and unexpected phenomena emerging from the complexity and connectivity of supermolecules. The most intriguing and challenging issues specific to supermolecules include vibrational coupling between the excited chromophore and its supramolecular surroundings, coherence transfer, and molecular design that would enable femtosecond electron transfer on a molecular level. It needs to be understood how imbedding of a photoactive species into a properly designed supermolecule can both accelerate photochemical reactions and increase their yields and selectivity [4,231,232]. General relations between supramolecular structure, dynamics and function will be sought. Much research interest will focus on early excited-state dynamics of photo-redox active dyads, triads, etc., dendrimers, host–guest complexes and other supramolecular assemblies, large polynuclear mixed-valence complexes, and multi-chromophoric arrays and multifunctional complexes capable of several distinct, simultaneous responses to optical excitation. Ligand-stabilized metal clusters and nanoparticles [233] will also attract attention.

Excitation with high-intensity femtosecond laser pulses can induce 2-photon ultrafast photochemistry and photophysics. Such processes have hardly been studied [48,234,235] for coordination and organometallic compounds. Nevertheless, they are potentially very important since chemistry of excited states inaccessible by conventional excitation may be explored [48]. Practically, it is of importance that

2-photon photochemistry of transition metal complexes can be initiated by low-energy red or near-infrared light.

Experimentally, much broader use of structure-sensitive methods (especially time-resolved resonance Raman and infrared spectroscopies) can be foreseen, namely to identify activated vibrations and structurally characterize excited states and reactive intermediates. Laser pulse excitation is a very convenient tool for a rapid generation of reactive species in high local concentrations. This is important for photocatalysis, photoinitiation and for mechanistic studies of chemical reactivity of coordinatively unsaturated molecules, complexes containing metals or ligands in unusual oxidation states, or radicals. Time-resolved spectroscopic techniques can reveal the structure and dynamics of these highly reactive chemical species and active catalysts, and determine kinetics of their reactions on a time scale ranging from femtoseconds to milliseconds. Activation of a C–H bond by ultrafast-generated Rh–monocarbonyls (as discussed above) provides a good example. Mechanistic studies of CO insertion into a metal–alkyl bond [236–238] or photochemical NO generation from metal nitrosyls [210,239], which has possible therapeutic applications, are another demonstrations of this approach. The flash-quench technique developed [240–242] to study electron-transfer in metalloproteins is based on a photochemical generation of strong oxidants or reductants by bimolecular electron transfer reactions of long-lived $^3\text{MLCT}$ excited states of $[\text{Ru}(\text{bpy})_3]^{2+}$. Recently, this technique has been developed further [243] by attaching a site-selective substrate to the 4-position of a bpy ligand. This allows the use of the flash-quench technique to study the redox chemistry of the deeply buried active site of cytochrome P450 metalloenzymes [243]. Similarly, dynamics of protein folding can be studied over a very broad time range using various laser-pulse generated redox agents [244]. A widespread use of photochemical laser-pulse initiation in mechanistic studies of thermal reactions and in the generation of complexes in unusual oxidation states is expected.

Investigations of photochemical reactions with the shortest available time-resolution is another important trend. Real-time dynamics of many initial photochemical steps, for which only upper limits are presently known, will be determined. The actual dynamics will probably significantly differ from conventional exponential-type kinetics. Direct comparison between experiments and calculated wave packet dynamics will be possible. These studies will also provide many more examples of coherent phenomena and unravel relations between coherence and photochemical dynamics.

Future applications of the photochemistry of coordination and organometallic compounds will utilize ultrafast processes as well as slower reactions of relaxed excited states. In fact, it can be advantageous to combine reactions occurring on these two time scales in a single process as nature does in photosynthesis and vision. Most promising applications are expected in broad fields of light energy conversion and information processing. Both these types of applications will require a purposeful design of molecular photonic materials, most probably based on supermolecules.

To this effect, a strongly multidisciplinary research connecting synthetic, material, and theoretical chemistry, photochemistry, spectroscopy and electrochemistry will be needed. On their way toward applications, mechanistic photochemists will have to shift their attention from solutions of photoactive compounds to films, layers, polymers, glasses or crystals.

Progress in light energy conversion can be expected to take place especially in development of photovoltaic cells based on sensitized semiconductors. The long-term stability of solvents and mediators used seems to be the main obstacle. Efficiency of light collection also needs to be improved. Construction of lamellar materials, in which photo- and redox-active layers are separated by inorganic layers represent another promising direction [245,246]. Such devices can utilize sensitizers with inherently long-lived excited states while the use of ultrafast electron injection would improve yields, rates and stability.

Possible applications in molecular electronics comprise design of new molecular photonic materials based on transition metal compounds and supermolecules. Such novel materials can be used for fluorescence-based sensors, optical-limiting, higher harmonic generation, photo- or electro-chromic devices or photo-switchable magnetic materials. However, the most challenging aspect of molecular electronics is the design and development of functional molecules and processes for photochemical storage, transfer, and manipulation of information. Molecular computing remains the ultimate, but still elusive, goal. It is a question to which extent is it promising to try to duplicate on a molecular level operations that are so well performed by solid-state silicon devices. Perhaps, an entirely new approach to molecular computing is needed. One may imagine that multichromophoric, multifunctional supermolecules could perform genuine quantum computing [247], possibly using coherence effects.

Acknowledgements

This work is part of a European COST D14 program. Support from the Ministry of Education of the Czech Republic (grant OC.D14.20) is much appreciated.

References

- [1] R.W. Schoenlein, L.A. Peteanu, R.A. Mathies, C.V. Shank, *Science* 254 (1991) 412.
- [2] R.W. Schoenlein, L.A. Peteanu, Q. Wang, R.A. Mathies, C.V. Shank, *J. Phys. Chem.* 97 (1993) 12087.
- [3] Q. Wang, R.W. Schoenlein, L.A. Peteanu, R.A. Mathies, C.V. Shank, *Science* 266 (1994) 422.
- [4] F. Gai, K.C. Hasson, J.C. McDonald, P.A. Anfinrud, *Science* 279 (1998) 1886.
- [5] V. Balzani, F. Scandola, *Supramolecular Photochemistry*, Ellis Horwood, Chichester, 1991.
- [6] P. Mathis, in: M. Chanon (Ed.), *Homogeneous Photocatalysis*, Wiley, New York, 1997, p. 355.
- [7] J. Barber, B. Andersson, *Nature* 370 (1994) 31.
- [8] A. Juris, V. Balzani, F. Barigelletti, S. Campagna, P. Belser, A. von Zelewsky, *Coord. Chem. Rev.* 84 (1988) 85.
- [9] N.H. Damrauer, G. Cerullo, A. Yeh, T.R. Boussie, C.V. Shank, J.K. McCusker, *Science* 275 (1997) 54.

- [10] B. Durham, J.V. Caspar, J.K. Nagle, T.J. Meyer, *J. Am. Chem. Soc.* 104 (1982) 4803.
- [11] T.J. Meyer, *Pure Appl. Chem.* 58 (1986) 1193.
- [12] (a) P.D. Fleischauer, A.W. Adamson, G. Sartori, *Progr. Inorg. Chem.* 17 (1972) 1. (b) A.W. Adamson, *Pure Appl. Chem.* 51 (1979) 313.
- [13] A.W. Adamson, in: K. Kalyanasundaram, M. Grätzel (Eds.), *Photosensitization and Photocatalysis Using Inorganic and Organometallic Compounds*, Kluwer, Dordrecht, 1993, p. 1.
- [14] B.R. Hollebone, C.H. Langford, N. Serpone, *Coord. Chem. Rev.* 39 (1981) 181.
- [15] A.J. Lees, *Chem. Rev.* 87 (1987) 711.
- [16] P.D. Beer, Z. Chen, A.J. Goulden, A. Grieve, D. Heseck, F. Szemes, T. Wear, *J. Chem. Soc. Chem. Commun.* (1994) 1269.
- [17] P.D. Beer, S.W. Dent, T.J. Wear, *J. Chem. Soc. Dalton Trans.* (1996) 2341.
- [18] R. Grigg, J.M. Holmes, S.K. Jones, W.D.J.A. Norbert, *J. Chem. Soc. Chem. Commun.* (1994) 185.
- [19] J.M. Price, W. Xu, J.N. Demas, B.A. DeGraff, *Anal. Chem.* 70 (1998) 265.
- [20] A.J. Lees, *Coord. Chem. Rev.* 177 (1998) 3.
- [21] G.L. Geoffroy, M.S. Wrighton, *Organometallic Photochemistry*, Academic Press, New York, 1979.
- [22] O. Horvath, K.L. Stevenson, *Charge Transfer Photochemistry of Coordination Compounds*, VCH, New York, 1993.
- [23] D.M. Roundhill, *Photochemistry and Photophysics of Metal Complexes*, Plenum Press, New York, 1994.
- [24] V. Balzani, V. Carassiti, *Photochemistry of Coordination Compounds*, Academic Press, London, 1970.
- [25] D.J. Stufkens, A. Vlček Jr., *Coord. Chem. Rev.* 177 (1998) 127.
- [26] J.K. Nagle, D.M. Roundhill, *Chemtracts Inorg. Chem.* 4 (1992) 141.
- [27] A.P. Zipp, *Coord. Chem. Rev.* 84 (1988) 47.
- [28] J.L. Marshall, A.E. Stiegman, H.B. Gray, in: A.B.P. Lever (Ed.), *Excited States and Reactive Intermediates*. ACS Symposium Series, vol. 307, American Chemical Society, Washington, DC, 1986, p. 166.
- [29] D.M. Roundhill, H.B. Gray, C.-M. Che, *Acc. Chem. Res.* 22 (1989) 55.
- [30] D.C. Smith, H.B. Gray, in: D.R. Salahub, M.C. Zerner (Eds.), *ACS Symposium Series 394. The Challenge of d and f Electrons*, American Chemical Society, Washington, DC, 1989, p. 356.
- [31] D.C. Smith, H.B. Gray, *Coord. Chem. Rev.* 100 (1990) 169.
- [32] R.J. Sweeney, E.L. Harvey, H.B. Gray, *Coord. Chem. Rev.* 105 (1990) 23.
- [33] S.F. Rice, H.B. Gray, *J. Am. Chem. Soc.* 105 (1983) 4571.
- [34] C.-M. Che, L.G. Butler, H.B. Gray, R.M. Crooks, W.H. Woodruff, *J. Am. Chem. Soc.* 105 (1983) 5492.
- [35] E.L. Harvey, A.E. Stiegman, A. Vlček Jr., H.B. Gray, *J. Am. Chem. Soc.* 109 (1987) 5233.
- [36] A. Vlček Jr., H.B. Gray, *J. Am. Chem. Soc.* 109 (1987) 286.
- [37] A. Vlček Jr., H.B. Gray, *Inorg. Chem.* 26 (1987) 1997.
- [38] J. Lin, C.U. Pittman Jr., *J. Organomet. Chem.* 512 (1996) 69.
- [39] W.A. Kalsbeck, D.M. Gingell, J.E. Malinsky, H.H. Thorp, *Inorg. Chem.* 33 (1994) 3313.
- [40] L.S. Fox, M. Kozik, J.R. Winkler, H.B. Gray, *Science* 247 (1990) 1069.
- [41] R.S. Farid, I.-J. Chang, J.R. Winkler, H.B. Gray, *J. Phys. Chem.* 98 (1994) 5176.
- [42] D. Wiedenfeld, M. Bachrach, T.M. McCleskey, M.G. Hill, H.B. Gray, J.R. Winkler, *J. Phys. Chem. B* 101 (1997) 8823.
- [43] I.V. Kurnikov, L.D. Zusman, M.G. Kurnikova, R.S. Farid, D.N. Beratan, *J. Am. Chem. Soc.* 119 (1997) 5690.
- [44] T.M. McCleskey, J.R. Winkler, H.B. Gray, *J. Am. Chem. Soc.* 114 (1992) 6935.
- [45] W.C. Trogler, H.B. Gray, *Acc. Chem. Res.* 11 (1978) 232.
- [46] V.M. Miskowski, R.A. Goldbeck, D.S. Kliger, H.B. Gray, *Inorg. Chem.* 18 (1979) 86.
- [47] M.D. Hopkins, H.B. Gray, *J. Am. Chem. Soc.* 106 (1984) 2468.
- [48] D.G. Nocera, *Acc. Chem. Res.* 28 (1995) 209.

- [49] D.G. Nocera, H.B. Gray, *J. Am. Chem. Soc.* 103 (1981) 7349.
- [50] A.M. Macintosh, D.G. Nocera, *Inorg. Chem.* 35 (1996) 7134.
- [51] K. Kalyanasundaram, *Photochemistry of Polypyridine and Porphyrin Complexes*, Academic Press, London, 1992.
- [52] J.R. Darwent, P. Douglas, A. Harriman, G. Porter, M.-C. Richoux, *Cood. Chem. Rev.* 44 (1982) 83.
- [53] A. Harriman, in: K. Kalyanasundaram, M. Grätzel (Eds.), *Photosensitization and Photocatalysis Using Inorganic and Organometallic Compounds*, Kluwer, Dordrecht, 1993, p. 273.
- [54] W. Paw, S.D. Cummings, M.A. Mansour, W.B. Connick, D.K. Geiger, R. Eisenberg, *Coord. Chem. Rev.* 171 (1998) 125.
- [55] J.A. Zuleta, M.S. Burberry, R. Eisenberg, *Coord. Chem. Rev.* 97 (1990) 47.
- [56] R. Ziessel, *Angew. Chem. Int. Ed. Engl.* 30 (1991) 844.
- [57] R. Ziessel, *J. Am. Chem. Soc.* 115 (1993) 118.
- [58] D. Sandrini, M. Maestri, R. Ziessel, *Inorg. Chim. Acta* 163 (1989) 177.
- [59] B.D. Rossenaar, M.W. George, F.P.A. Johnson, D.J. Stufkens, J.J. Turner, A. Vlček Jr., *J. Am. Chem. Soc.* 117 (1995) 11582.
- [60] B.D. Rossenaar, C.J. Kleverlaan, M.C.E. van de Ven, D.J. Stufkens, A. Vlček Jr., *Chem.-Eur. J.* 2 (1996) 228.
- [61] M.P. Aarnts, D.J. Stufkens, M.P. Wilms, E.J. Baerends, A. Vlček Jr., I.P. Clark, M.W. George, J.J. Turner, *Chem.-Eur. J.* 2 (1996) 1556.
- [62] C.J. Kleverlaan, D.J. Stufkens, I.P. Clark, M.W. George, J.J. Turner, D.M. Martino, H. van Willigen, A. Vlček Jr., *J. Am. Chem. Soc.* 120 (1998) 10871.
- [63] I.R. Farrell, P. Matousek, C.J. Kleverlaan, A. Vlček, Jr., *Chem.-Eur. J.* 6 (2000) 1386.
- [64] D.A. Sexton, L.H. Skibsted, D. Magde, P.C. Ford, *J. Phys. Chem.* 86 (1982) 1758.
- [65] V. Balzani, F. Bolletta, M.T. Gandolfi, M. Maestri, *Top. Curr. Chem.* 75 (1978) 1.
- [66] V. Balzani, F. Bolletta, F. Scandola, R. Ballardini, *Pure Appl. Chem.* 51 (1979) 299.
- [67] V. Balzani, F. Bolletta, *Comments Inorg. Chem.* 2 (1983) 211.
- [68] K. Kalyanasundaram, in: K. Kalyanasundaram, M. Grätzel (Eds.), *Photosensitization and Photocatalysis Using Inorganic and Organometallic Compounds*, Kluwer, Dordrecht, 1993, p. 113.
- [69] H.D. Gafney, A.W. Adamson, *J. Am. Chem. Soc.* 94 (1972) 8238.
- [70] M. Ruthkosky, C.A. Kelly, F.N. Castellano, G.J. Meyer, *Coord. Chem. Rev.* 171 (1998) 309.
- [71] J.V. Caspar, T.J. Meyer, *J. Phys. Chem.* 87 (1983) 952.
- [72] E.M. Kober, J.V. Caspar, R.S. Lumpkin, T.J. Meyer, *J. Phys. Chem.* 90 (1986) 3722.
- [73] J.V. Caspar, T.J. Meyer, *Inorg. Chem.* 22 (1983) 2444.
- [74] J.V. Caspar, E.M. Kober, B.P. Sullivan, T.J. Meyer, *J. Am. Chem. Soc.* 104 (1982) 630.
- [75] G.F. Strouse, J.R. Schoonover, R. Duesing, S. Boyde, W.E. Jones, T.J. Meyer, *Inorg. Chem.* 34 (1995) 473.
- [76] J.A. Treadway, B. Loeb, R. Lopez, P.A. Anderson, F.R. Keene, T.J. Meyer, *Inorg. Chem.* 35 (1996) 2242.
- [77] P. Chen, T.J. Meyer, *Chem. Rev.* 98 (1998) 1439.
- [78] L. De Cola, F. Barigelletti, V. Balzani, P. Belser, A. von Zelewsky, F. Vögtle, F. Ebmeyer, S. Grammenudi, *J. Am. Chem. Soc.* 110 (1988) 7210.
- [79] F. Barigelletti, L. De Cola, V. Balzani, P. Belser, A. von Zelewsky, F. Vögtle, F. Ebmeyer, S. Grammenudi, *J. Am. Chem. Soc.* 111 (1989) 4662.
- [80] M. Hissler, A. Harriman, A. Khatyr, R. Ziessel, *Chem. Eur. J.* 5 (1999) 3366.
- [81] L. Hammarström, F. Barigelletti, L. Flamigni, M.T. Indelli, N. Armaroli, G. Calogero, M. Guardigli, A. Sour, J.-P. Collin, J.-P. Sauvage, *J. Phys. Chem. A* 101 (1997) 9061.
- [82] A. Harriman, R. Ziessel, *Coord. Chem. Rev.* 171 (1998) 331.
- [83] A. Harriman, R. Ziessel, *Chem. Commun.* (1996) 1707.
- [84] C. Berg-Brennan, P. Subramanian, M. Absi, C. Stern, J.T. Hupp, *Inorg. Chem.* 35 (1996) 3719.
- [85] R. Ziessel, A. Juris, M. Venturi, *Chem. Commun.* (1997) 1593.
- [86] R. Ziessel, A. Juris, M. Venturi, *Inorg. Chem.* 37 (1998) 5061.
- [87] P. Lainé, E. Amouyal, *Chem. Comm.* (1999) 935.
- [88] M. Grätzel, *Acc. Chem. Res.* 14 (1981) 376.
- [89] E. Borgarello, J. Kiwi, E. Pelizzetti, M. Visca, M. Grätzel, *Nature* 289 (1981) 158.

- [90] A.J. Bard, M.A. Fox, *Acc. Chem. Res.* 28 (1995) 141.
- [91] E. Amouyal, *Sol. Energy Mater. Sol. Cells* 38 (1995) 249.
- [92] K. Kalyanasundaram, M. Grätzel, *Coord. Chem. Rev.* 177 (1998) 347.
- [93] M. Grätzel, *Coord. Chem. Rev.* 111 (1991) 167.
- [94] B. O'Regan, M. Grätzel, *Nature* 353 (1991) 737.
- [95] Y. Tachibana, J.E. Moser, M. Grätzel, D.R. Klug, J.R. Durrant, *J. Phys. Chem.* 100 (1996) 20056.
- [96] J.M. Rehm, G.L. McLendon, Y. Nagasawa, K. Yoshihara, J. Moser, M. Grätzel, *J. Phys. Chem.* 100 (1996) 9577.
- [97] B. Burfeindt, T. Hannappel, W. Storck, F. Willig, *J. Phys. Chem.* 100 (1996) 16463.
- [98] S. Ferrere, B.A. Gregg, *J. Am. Chem. Soc.* 120 (1998) 843.
- [99] I.R. Farrell, A. Vlček, Jr., *Coord. Chem. Rev.*, in press.
- [100] I.R. Farrell, P. Matousek, A. Vlček Jr., *J. Am. Chem. Soc.* 121 (1999) 5296.
- [101] N.H. Damrauer, J.K. McCusker, *J. Phys. Chem. A* 103 (1999) 8440.
- [102] J.K. McCusker, K.N. Walda, R.C. Dunn, J.D. Simon, D. Magde, D.N. Hendrickson, *J. Am. Chem. Soc.* 115 (1993) 298.
- [103] P. Gütllich, A. Hauser, H. Spiering, *Angew. Chem. Int. Ed. Engl.* 33 (1994) 2024.
- [104] A. Hauser, J. Jęftić, H. Romstedt, R. Hinek, H. Spiering, *Coord. Chem. Rev.* 190–192 (1999) 471.
- [105] J.K. McCusker, K.N. Walda, D. Magde, D.N. Hendrickson, *Inorg. Chem.* 32 (1993) 394.
- [106] M.D. Edington, W.M. Diffey, W.J. Doria, R.E. Riter, W.F. Beck, *Chem. Phys. Lett.* 275 (1997) 119.
- [107] R. Lingle Jr., X. Xu, H. Zhu, S.-C. Yu, J.B. Hopkins, *J. Phys. Chem.* 95 (1991) 9320.
- [108] M. Lim, T.A. Jackson, P.A. Anfinrud, *J. Phys. Chem.* 100 (1996) 12043.
- [109] L.C. Abbott, C.J. Arnold, T.-Q. Ye, K.C. Gordon, R.N. Perutz, R.E. Hester, J.N. Moore, *J. Phys. Chem. A* 102 (1998) 1252.
- [110] J.R. Hill, C.J. Ziegler, K.S. Suslick, D.D. Dlott, C.W. Rella, M.D. Fayer, *J. Phys. Chem.* 100 (1996) 18023.
- [111] T.P. Dougherty, W.T. Grubbs, E.J. Heilweil, *J. Phys. Chem.* 98 (1994) 9396.
- [112] S.J. Rosenthal, X. Xie, M. Du, G.R. Fleming, *J. Chem. Phys.* 95 (1991) 4715.
- [113] P.F. Barbara, W. Jarzeba, *Adv. Photochem.* 15 (1990) 1.
- [114] J.L. Pogge, D.F. Kelley, *Chem. Phys. Lett.* 238 (1995) 16.
- [115] J.P. Cushing, C. Butoi, D.F. Kelley, *J. Phys. Chem. A* 101 (1997) 7222.
- [116] Y. Mizutani, T. Kitagawa, *Science* 278 (1997) 443.
- [117] L. Zhu, T. Sage, P.M. Champion, *Science* 266 (1994) 629.
- [118] L.D. Book, D.C. Arnett, H. Hu, N.F. Scherer, *J. Phys. Chem. A* 102 (1998) 4350.
- [119] R.J. Ellingson, J.B. Asbury, S. Ferrere, H.N. Ghosh, J.R. Sprague, T. Lian, A.J. Nozik, *J. Phys. Chem. B* 102 (1998) 6455.
- [120] J.B. Asbury, R.J. Ellingson, H.N. Ghosh, S. Ferrere, A.J. Nozik, T. Lian, *J. Phys. Chem. B* 103 (1999) 3110.
- [121] T. Hannappel, B. Burfeindt, W. Storck, F. Willig, *J. Phys. Chem. B* 101 (1997) 6799.
- [122] H.N. Ghosh, J.B. Asbury, Y. Weng, T. Lian, *J. Phys. Chem. B* 102 (1998) 10208.
- [123] N.J. Cherepy, G.P. Smestad, M. Grätzel, J.Z. Zhang, *J. Phys. Chem. B* 101 (1997) 9342.
- [124] M. Hilgendorff, V. Sundström, *J. Phys. Chem. B* 102 (1998) 10505.
- [125] H.N. Ghosh, J.B. Asbury, T. Lian, *J. Phys. Chem. B* 102 (1998) 6482.
- [126] R.L. Blackburn, C.S. Johnson, J.T. Hupp, *J. Am. Chem. Soc.* 113 (1991) 1060.
- [127] Y. Tachibana, S.A. Haque, I.P. Mercer, J.R. Durrant, D.R. Klug, *J. Phys. Chem. B* 104 (2000) 1198.
- [128] M. Hilgendorff, V. Sundström, *Chem. Phys. Lett.* 287 (1998) 709.
- [129] V. Balzani, F. Scandola, in: D.N. Reinhoudt (Ed.), *Comprehensive Supramolecular Chemistry*, vol. 10, Elsevier Science, Oxford, 1996, p. 687.
- [130] V. Balzani, S. Campagna, G. Denti, A. Juris, S. Serroni, M. Venturi, *Acc. Chem. Res.* 31 (1998) 26.
- [131] E.H. Yonemoto, G.B. Saupe, R.H. Schmehl, S.M. Hubig, R.L. Riley, B.L. Iverson, T.E. Mallouk, *J. Am. Chem. Soc.* 116 (1994) 4786.

- [132] J.-C. Chambron, A. Harriman, V. Heitz, J.-P. Sauvage, *J. Am. Chem. Soc.* 115 (1993) 6109.
- [133] D. LeGourriérec, M. Andersson, J. Davidsson, E. Mukhtar, L. Sun, L. Hammarström, *J. Phys. Chem. A* 103 (1999) 557.
- [134] M.D. Ward, *Chem. Soc. Rev.* 26 (1997) 365.
- [135] J.-P. Collin, A. Harriman, V. Heitz, F. Odobel, J.-P. Sauvage, *J. Am. Chem. Soc.* 116 (1994) 5679.
- [136] J.-P. Collin, P. Gaviña, V. Heitz, J.-P. Sauvage, *Eur. J. Inorg. Chem.* (1998) 1.
- [137] J.-C. Chambron, A. Harriman, V. Heitz, J.-P. Sauvage, *J. Am. Chem. Soc.* 115 (1993) 7419.
- [138] P. Chen, M. Curry, T.J. Meyer, *Inorg. Chem.* 28 (1989) 2271.
- [139] J.R. Schoonover, P. Chen, W.D. Bates, R.B. Dyer, T.J. Meyer, *Inorg. Chem.* 33 (1994) 793.
- [140] D.J. Liard, A. Vlček, Jr., *Inorg. Chem.* 39 (2000) 485.
- [141] V. Grossshenny, A. Harriman, R. Ziessel, *Angew. Chem. Int. Ed. Engl.* 34 (1995) 2705.
- [142] R. Ziessel, M. Hissler, A. El-ghayoury, A. Harriman, *Coord. Chem. Rev.* 178–180 (1998) 1251.
- [143] L. De Cola, P. Belser, *Coord. Chem. Rev.* 177 (1998) 301.
- [144] M. Andersson, J. Davidsson, L. Hammarström, J. Korppi-Tommola, T. Peltola, *J. Phys. Chem. B* 103 (1999) 3258.
- [145] H. Chosrowjan, S. Taniguchi, T. Okada, S. Takagi, T. Arai, K. Tokumaru, *Chem. Phys. Lett.* 242 (1995) 644.
- [146] I.V. Rubtsov, H. Shirota, K. Yoshihara, *J. Phys. Chem. A* 103 (1999) 1801.
- [147] S. Engleitner, M. Seel, W. Zinth, *J. Phys. Chem. A* 103 (1999) 3013.
- [148] P. Gilch, F. Pöllinger-Dammer, C. Musewald, M.E. Michel-Beyerle, U.E. Steiner, *Science* 281 (1998) 982.
- [149] G.C. Walker, P.F. Barbara, S.K. Doorn, Y. Dong, J.T. Hupp, *J. Phys. Chem.* 95 (1991) 5712.
- [150] S.K. Doorn, P.O. Stoutland, R.B. Dyer, W.H. Woodruff, *J. Am. Chem. Soc.* 114 (1992) 3133.
- [151] S.K. Doorn, R.B. Dyer, P.O. Stoutland, W.H. Woodruff, *J. Am. Chem. Soc.* 115 (1993) 6398.
- [152] K. Tominaga, D.A.V. Kliner, A.E. Johnson, N.E. Levinger, P.F. Barbara, *J. Chem. Phys.* 98 (1993) 1228.
- [153] P.J. Reid, C. Silva, P.F. Barbara, L. Karki, J.T. Hupp, *J. Phys. Chem.* 99 (1995) 2609.
- [154] D.C. Arnett, P. Vöhringer, N.F. Scherer, *J. Am. Chem. Soc.* 117 (1995) 12262.
- [155] O. Sato, T. Iyoda, A. Fujishima, K. Hashimoto, *Science* 272 (1996) 704.
- [156] K.G. Spears, X. Wen, R. Zhang, *J. Phys. Chem.* 100 (1996) 10206.
- [157] V. Balzani, A. Juris, M. Venturi, S. Campagna, S. Serroni, *Chem. Rev.* 96 (1996) 759.
- [158] F. Scandola, C.A. Bignozzi, M.T. Indelli, in: K. Kalyanasundaram, M. Grätzel (Eds.), *Photosensitization and Photocatalysis Using Inorganic and Organometallic Compounds*, Kluwer, Dordrecht, 1993, p. 161.
- [159] B. Schlicke, P. Belser, L. De Cola, E. Sabbioni, V. Balzani, *J. Am. Chem. Soc.* 121 (1999) 4207.
- [160] J.-S. Hsiao, B.P. Krueger, R.W. Wagner, T.E. Johnson, J.K. Delaney, D.C. Mauzerall, G.R. Fleming, J.S. Lindsey, D.F. Bocian, R.J. Donohoe, *J. Am. Chem. Soc.* 118 (1996) 11181.
- [161] J. Li, A. Ambrose, S.I. Yang, J.R. Diers, J. Seth, C.R. Wack, D.F. Bocian, D. Holten, J.S. Lindsey, *J. Am. Chem. Soc.* 121 (1999) 8927.
- [162] P. Hascoat, S.I. Yang, R.K. Lammi, J. Alley, D.F. Bocian, J.S. Lindsey, D. Holten, *Inorg. Chem.* 38 (1999) 4849.
- [163] P. Brodard, S. Matzinger, E. Vauthey, O. Mongin, C. Papamicaël, A. Gossauer, *J. Phys. Chem. A* 103 (1999) 5858.
- [164] V. Balzani, F. Bolletta, F. Scandola, *J. Am. Chem. Soc.* 102 (1980) 2152.
- [165] V. Balzani, M. Maestri, in: K. Kalyanasundaram, M. Grätzel (Eds.), *Photosensitization and Photocatalysis Using Inorganic and Organometallic Compounds*, Kluwer, Dordrecht, 1993, p. 15.
- [166] L. Flamigni, F. Barigelletti, N. Armaroli, B. Ventura, J.-P. Collin, J.-P. Sauvage, J.A.G. Williams, *Inorg. Chem.* 38 (1999) 661.
- [167] A. Harriman, F.M. Romero, R. Ziessel, A.C. Benniston, *J. Phys. Chem. A* 103 (1999) 5399.
- [168] A. Harriman, M. Hissler, O. Trompette, R. Ziessel, *J. Am. Chem. Soc.* 121 (1999) 2516.
- [169] L. Khundkar, A.H. Zewail, *Annu. Rev. Phys. Chem.* 41 (1990) 15.
- [170] A.H. Zewail, *J. Phys. Chem.* 97 (1993) 12427.
- [171] N. Pugliano, S. Gnanakaran, R.M. Hochstrasser, *J. Photochem. Photobiol. A: Chem.* 102 (1996) 21.

- [172] T. Lian, S.E. Bromberg, M.C. Asplund, H. Yang, C.B. Harris, *J. Phys. Chem.* 100 (1996) 11994.
- [173] E.J. Baerends, A. Rosa, *Coord. Chem. Rev.* 177 (1998) 97.
- [174] C. Pollak, A. Rosa, E.J. Baerends, *J. Am. Chem. Soc.* 119 (1997) 7324.
- [175] A. Rosa, E.J. Baerends, S.J.A. van Gisbergen, E. van Lenthe, J.A. Groeneveld, J.G. Snijders, *J. Am. Chem. Soc.* 121 (1999) 10356.
- [176] D.P. Drolet, A.J. Lees, *J. Am. Chem. Soc.* 114 (1992) 4186.
- [177] A.A. Purwoko, A.J. Lees, *Inorg. Chem.* 34 (1995) 424.
- [178] A.A. Purwoko, S.D. Tibensky, A.J. Lees, *Inorg. Chem.* 35 (1996) 7049.
- [179] A.A. Purwoko, A.J. Lees, *Inorg. Chem.* 35 (1996) 675.
- [180] N. Dunwoody, A.J. Lees, *Organometallics* 16 (1997) 5770.
- [181] A.J. Lees, *J. Organomet. Chem.* 554 (1998) 1.
- [182] H. Yang, K.T. Kotz, M.C. Asplund, M.J. Wilkens, C.B. Harris, *Acc. Chem. Res.* 32 (1999) 551.
- [183] S.E. Bromberg, T. Lian, R.G. Bergman, C.B. Harris, *J. Am. Chem. Soc.* 118 (1996) 2069.
- [184] J.B. Asbury, H.N. Ghosh, J.S. Yeston, R.G. Bergman, T. Lian, *Organometallics* 17 (1998) 3417.
- [185] T. Lian, S.E. Bromberg, H. Yang, G. Proulx, R.G. Bergman, C.B. Harris, *J. Am. Chem. Soc.* 118 (1996) 3769.
- [186] S.E. Bromberg, H. Yang, M.C. Asplund, T. Lian, B.K. McNamara, K.T. Kotz, J.S. Yeston, M. Wilkens, H. Frei, R.G. Bergman, C.B. Harris, *Science* 278 (1997) 260.
- [187] H. Yang, K.T. Kotz, M.C. Asplund, C.B. Harris, *J. Am. Chem. Soc.* 119 (1997) 9564.
- [188] H. Yang, M.C. Asplund, K.T. Kotz, M.J. Wilkens, H. Frei, C.B. Harris, *J. Am. Chem. Soc.* 120 (1998) 10154.
- [189] A. Vlček Jr., J. Vichová, F. Hartl, *Coord. Chem. Rev.* 132 (1994) 167.
- [190] A. Vlček Jr., *Coord. Chem. Rev.* 177 (1998) 219.
- [191] R.W. Balk, T. Snoeck, D.J. Stufkens, A. Oskam, *Inorg. Chem.* 19 (1980) 3015.
- [192] S. Wieland, K.B. Reddy, R. van Eldik, *Organometallics* 9 (1990) 1802.
- [193] W.F. Fu, R. van Eldik, *Inorg. Chim. Acta* 251 (1996) 341.
- [194] W.-F. Fu, R. van Eldik, *Inorg. Chem.* 37 (1998) 1044.
- [195] J. Vichová, F. Hartl, A. Vlček Jr., *J. Am. Chem. Soc.* 114 (1992) 10903.
- [196] I.G. Virrels, M.W. George, J.J. Turner, J. Peters, A. Vlček Jr., *Organometallics* 15 (1996) 4089.
- [197] D. Guillaumont, C. Daniel, A. Vlček Jr., *Inorg. Chem.* 36 (1997) 1684.
- [198] D. Guillaumont, C. Daniel, A. Vlček, Jr., *J. Phys. Chem. A* (2000), in press.
- [199] G.J. Stor, S.L. Morrison, D.J. Stufkens, A. Oskam, *Organometallics* 13 (1994) 2641.
- [200] G.J. Stor, D.J. Stufkens, P. Vernooijs, E.J. Baerends, J. Fraanje, K. Goubitz, *Inorg. Chem.* 34 (1995) 1588.
- [201] C.J. Kleverlaan, F. Hartl, D.J. Stufkens, *J. Photochem. Photobiol. A: Chem.* 103 (1997) 231.
- [202] A. Rosa, G. Ricciardi, E.J. Baerends, D.J. Stufkens, *J. Phys. Chem.* 100 (1996) 15346.
- [203] I.R. Farrell, P. Matousek, A. Vlček, Jr., *Inorg. Chem.*, submitted for publication.
- [204] T. Kobayashi, H. Ohtani, H. Noda, S. Teratani, H. Yamazaki, K. Yasufuku, *Organometallics* 5 (1986) 110.
- [205] T. Kobayashi, K. Yasufuku, J. Iwai, H. Yesaka, H. Noda, H. Ohtani, *Coord. Chem. Rev.* 64 (1985) 1.
- [206] J.Z. Zhang, C.B. Harris, *J. Chem. Phys.* 95 (1991) 4024.
- [207] S.K. Kim, S. Pedersen, A.H. Zewail, *Chem. Phys. Lett.* 233 (1995) 500.
- [208] A. Rosa, G. Ricciardi, E.J. Baerends, D.J. Stufkens, *Inorg. Chem.* 35 (1996) 2886.
- [209] D.J. Stufkens, M.P. Aarnts, B.D. Rossenaar, A. Vlček Jr., *Pure Appl. Chem.* 69 (1997) 831.
- [210] E.A. Morlino, L.A. Walker II, R.J. Sension, M.A.J. Rodgers, *J. Am. Chem. Soc.* 117 (1995) 4429.
- [211] T.P. Causgrove, R.B. Dyer, *J. Phys. Chem.* 100 (1996) 3273.
- [212] M. Lim, T.A. Jackson, P.A. Anfinrud, *Science* 269 (1995) 962.
- [213] R. Osman, R.N. Perutz, A.D. Rooney, A.J. Langley, *J. Phys. Chem.* 98 (1994) 3562.
- [214] M. Colombo, M.W. George, J.N. Moore, D.I. Pattison, R.N. Perutz, I.G. Virrels, T.-Q. Ye, *J. Chem. Soc. Dalton Trans.* (1997) 2857.
- [215] C. Daniel, E. Kolba, L. Lehr, J. Manz, T. Schröder, *J. Phys. Chem.* 98 (1994) 9823.
- [216] C. Daniel, M.-C. Heitz, L. Lehr, J. Manz, T. Schröder, *J. Phys. Chem.* 97 (1993) 12485.

- [217] M.-C. Heitz, C. Daniel, *J. Am. Chem. Soc.* 119 (1997) 8269.
- [218] K. Finger, C. Daniel, *J. Am. Chem. Soc.* 117 (1995) 12322.
- [219] K. Finger, C. Daniel, P. Saalfrank, B. Schmidt, *J. Phys. Chem.* 100 (1996) 3368.
- [220] D. Guillaumont, C. Daniel, *J. Am. Chem. Soc.* 121 (1999) 11733.
- [221] D. Guillaumont, C. Daniel, manuscript in preparation.
- [222] C. Daniel, D. Guillaumont, C. Ribbing, B. Minaev, *J. Phys. Chem. A* 103 (1999) 5766.
- [223] C. Daniel, M.-C. Heitz, J. Manz, C. Ribbing, *J. Chem. Phys.* 102 (1995) 905.
- [224] C. Daniel, M.C. Heitz, L. Lehr, T. Schröder, B. Warmuth, *Int. J. Quant. Chem.* 52 (1994) 71.
- [225] M.C. Heitz, K. Finger, C. Daniel, *Coord. Chem. Rev.* 159 (1997) 171.
- [226] D. Guillaumont, K. Finger, M.R. Hachey, C. Daniel, *Coord. Chem. Rev.* 171 (1998) 439.
- [227] D. Guillaumont, C. Daniel, *Coord. Chem. Rev.* 177 (1998) 181.
- [228] A. Rosa, G. Ricciardi, E.J. Baerends, D.J. Stufkens, *Inorg. Chem.* 37 (1998) 6244.
- [229] N.S. Hush, J.R. Reimers, *Coord. Chem. Rev.* 177 (1998) 37.
- [230] A. Vogler, H. Kunkely, *Coord. Chem. Rev.* 177 (1998) 81.
- [231] H. Tributsch, L. Pohlmann, *Science* 279 (1998) 1891.
- [232] H. Tributsch, L. Pohlmann, *J. Electroanal. Chem.* 438 (1997) 37.
- [233] J.Z. Zhang, *Acc. Chem. Res.* 30 (1997) 423.
- [234] F.N. Castellano, H. Malak, I. Gryczynski, J.R. Lakowicz, *Inorg. Chem.* 36 (1997) 5548.
- [235] D.S. Engebretson, J.M. Zaleski, G.E. Leroi, D.G. Nocera, *Science* 265 (1994) 759.
- [236] W.T. Boese, P.C. Ford, *Organometallics* 13 (1994) 3525.
- [237] W.T. Boese, P.C. Ford, *J. Am. Chem. Soc.* 117 (1995) 8381.
- [238] W.T. Boese, K. McFarlane, B. Lee, J. Rabor, P.C. Ford, *Coord. Chem. Rev.* 159 (1997) 135.
- [239] P.C. Ford, J. Bourassa, K. Miranda, B. Lee, I. Lorkovic, S. Boggs, S. Kudo, L. Laverman, *Coord. Chem. Rev.* 171 (1998) 185.
- [240] J.R. Winkler, H.B. Gray, *Chem. Rev.* 92 (1992) 369.
- [241] H.B. Gray, W.R. Ellis Jr., in: I. Bertini, H.B. Gray, S.J. Lippard, J.S. Valentine (Eds.), *Bioinorganic Chemistry*, University Science Books, Mill Valley, CA, 1994, p. 315.
- [242] H.B. Gray, J.R. Winkler, *Annu. Rev. Biochem.* 65 (1996) 537.
- [243] J.J. Wilker, I.J. Dmochowski, J.H. Dawson, J.R. Winkler, H.B. Gray, *Angew. Chem. Int. Ed.* 38 (1999) 90.
- [244] J.R. Telford, P. Wittung-Stafshede, H.B. Gray, J.R. Winkler, *Acc. Chem. Res.* 31 (1998) 755.
- [245] D.M. Kaschak, S.A. Johnson, C.C. Waraksa, J. Pogue, T.E. Mallouk, *Coord. Chem. Rev.* 185–186 (1999) 403.
- [246] D.M. Kaschak, J.T. Lean, C.C. Waraksa, G.B. Saupe, H. Usami, T.E. Mallouk, *J. Am. Chem. Soc.* 121 (1999) 3435.
- [247] S. Lloyd, *Science* 261 (1993) 1569.
- [248] D. Guillaumont, M.P. Wilms, C. Daniel, D.J. Stufkens, *Inorg. Chem.* 37 (1998) 5816.